RGNZ/MGPB

The Impact of Geological and Rainfall Characteristics on Slope Stability Analysis in Shallow Landslide Modelling using the TRIGRS Model

Rudarsko-geološko-naftni zbornik
(The Mining-Geology-Petroleum Engineering Bulletin)
UDC: 551.3:551.5
DOI: 10.17794/rgn.2023.4.12

Preliminary communication

Khori Sugianti[1*] and Adrin Tohari[2]

[1] *Research Center for Geological Disaster, National Research and Innovation Agency (BRIN), Jl. Sangkuriang, Dago, Bandung, West Java, Indonesia 40135 ORCID 0000-0001-7990-7905.*

[2] *Research Center for Geological Disaster, National Research and Innovation Agency (BRIN), Jl. Sangkuriang, Dago, Bandung, West Java, Indonesia 40135 ORCID 0000-0002-6662-0697.*

Abstract

West Java Province has a high potential for susceptibility to landslides. West Bandung Regency is one of the regions in West Java which has high occurrences of landslides triggered by rainfalls. Rainfall-induced landslides in this region have occurred 165 times during rainfall in the last ten (10) years. An effort to predict the landslide occurrences in this region requires the knowledge of factors affecting the hillslope stability. This paper aims to (1) evaluate the parameters affecting slope stability, (2) determine rainfall characteristics affecting slope, and (3) evaluate the performance of TRIGRS modelling. This study applies a deterministic method using the model of TRIGRS to analyze the effect of one-day antecedent rainfall intensity on the instability of hillslopes. The parameters used in this study are based on field investigation, geological and topographical maps, soil engineering properties, and historical rainfall data. The effect of one-day antecedent rainfall intensity was considered in two scenarios, i.e. 6 hours and 12 hours of antecedent rainfall. Modelling results show that hillslope instability in the study areas is affected by many factors, such as hilly morphology, steep slopes, low shear strength parameters, weathering of volcanic rocks, and the lineament density of geological structures. The modelling simulation also indicates that landslide occurrences in this study area are initiated by a long antecedent rainfall period. Based on ROC analysis, the TRIGRS model shows that the model performance evaluation is in good agreement for modelling slope stability against actual landslide events.

Keywords:
landslide; antecedent rainfall; Gumbel method; slope stability; TRIGRS model

1. Introduction

In Indonesia, landslides are geological disasters that often occur. Landslides are widespread during long periods of heavy rain (**Tohari, 2018**). The main parameter that triggers landslides is rainfall (**Polemio and Petrucci, 2000; Farahmand and Kouchak, 2013**). Landslides triggered by rain are generally shallow (**Lepore et al., 2012; Tranet al., 2017**) and are associated with reduced shear strength soils and soil weathering grade (**Sugianti et al., 2022**). Rain infiltration induces a rise in groundwater tables and causes the soil to saturate due to increased pore water pressure, causing a reduction of soil strength properties and decreasing slope stability, thus triggering landslides (**Iverson, 2000**).

The efforts to minimize landslide risk require a better understanding of rainfall intensity characteristics as triggering factors of landslides. Researchers have studied the correlation between the characteristics of rainfall and landslide events as fundamental to determining and developing the warning system for real-time regional landslides (**Lateh et al., 2013; Hong et al., 2018**). The increase in rainfall intensity as a triggering factor for landslides causes an additional load on the slopes and an increase in pore-water pressure (**Iverson, 2000; Muntohar and Liao, 2008**). Landslides can occur even over long periods of rainfall, and the rainfall intensity will be lower due to the effect of previous rainfall (**Huang and Lin, 2002; Bai et al., 2014**). Landslide disasters can cause natural damage, social and economic losses, injuries, and deaths (**Turner, 2018; Aristizábal and Sánchez, 2020**). Mitigation and preparedness efforts to reduce landslide risk require analysis of slope stability in landslide risk areas and awareness of the causes of slope instability.

West Java Province has a high potential for susceptibility to landslides. The West Bandung Regency in West Java has the highest landslide hazard triggered by heavy rainfall. Regarding the landslide susceptibility map for West Java of the Geological Agency, Center for Volcanology and Geological Hazard Mitigation from Indonesia, the West Bandung area has a medium to high level

Corresponding author: Khori Sugianti
e-mail address: khorisugianti@gmail.com

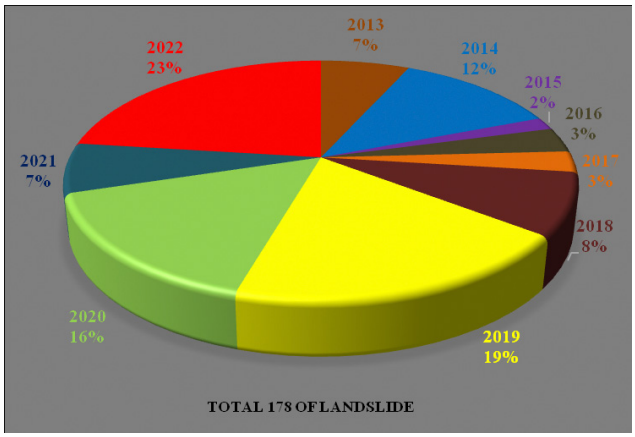

Figure 1: Landslide occurrence pattern for the last 10 years in West Bandung (https://dibi.bnpb.go.id/home/index2).

of susceptibility. **Figure 1** shows that landslides occurred 178 times in the West Bandung area during rainfall in one decade. So, landslide disasters have occurred almost yearly in the last decade in this region. Thus, to minimize the landslide hazard risk in West Bandung, knowledge of how rainfall influences landslide susceptibility in this region is necessary. This knowledge is obtained through a spatial landslide susceptibility modelling study.

Previous researchers have carried out various modelling using GIS (Geographical Information System) methods for landslide susceptibility. Several studies, including **Lee and Sambath (2006), and Chauhan et al. (2010)** used a logistic regression method that related the probability of landslide occurrence to independent variable parameters and the analytical hierarchy process (AHP) methods that consider many objective and subjective factors in ranking weighting (**Hadji et al., 2018; Zhao et al., 2017**) in statistical approaches to create landslide hazard zone maps. Other research has been conducted to map landslide hazards using the weighted value method (**Sugianti et al., 2014).** Models of probabilistic evaluation utilize multiple logistic regression analysis (**Kawagoe et al., 2010; Lee and Pradhan, 2006).** Landslide susceptibility statistical models highly depend on the input data of historical landslides. Some studies also focused on the landslide processes using the deterministic approach to predict regional-scale landslides (**Baum et al., 2005; Simoni et al., 2008).**

According to the landslide mechanism, rainfall infiltration can cause an increase in pore-water pressure from negative to positive pore-water pressure on shallow landslides. The role of rainwater infiltration in slope stability is very complex (**Tran et al., 2017**). Previous research combines a model of the physical-based model and the hydrogeological model for mapping shallow slope stability triggered by rainwater infiltration, such as the SINMAP, SHALSTAB, TRIGRS, GEOtop-FS, and TiVaSS models. The SINMAP considers a model of the parallel failure plane to the soil surface that calculates the stability of an infinite slope that complements the stability of gravity, soil shear angle, and cohesion in the failure plane on the soil surface of the slope (**Kawagoe et al., 2010**). The SHALSTAB model combines the analysis of infinite slope stability and the model of a steady-state hydrological condition for assessment areas with the potential for landslides (**Pack et al., 1998**). The GEOtop FS method is the most complex physics model based on the prediction of landslide susceptibility spatially and temporally by involving an association of two-dimensional surface runoff with three-dimensional unsaturated subsurface flow (**Dietrich et al., 1998**). The development of TRIGRS is based on a one-dimensional model of vertical infiltration to predict the simple stability of an infinite slope (**Baum et al., 2005**). Meanwhile, the TiVaSS model is a physically based model that uses Richards' 3-D formulation and stability of the infinite slope basic equation for landslides of shallow depth due to rainfall (**Simoni et al., 2008**).

In order to predict the susceptibility of hillslopes to rainfall-triggered shallow landslides, the TRIGRS model - a grid-based regional slope stability model, is most commonly used (**Baum et al., 2002**). TRIGRS calculates the change of the transient pore pressure and an attendant change in the slope safety factor due to rainfall infiltration using the linearized Richards formula by **Iverson (2000)** and **Baum et al. (2002)**. In contrast, other physical models do not consider the transient transformation of saturation induced by rainfall infiltration (**Baum et al., 2002**). The advantage of TRIGRS is that the model is capable of estimating trigger factors that are sensitive to landslides (**Baum et al., 2010**), zoning susceptibility maps (**Pack et al., 2013; Sugianti et al., 2016**), and predicting landslides (**Zhuang et al., 2017**). Although previous studies have shown that the TRIGRS performance is comparable with other models, such as the TiVaSS (**Tran et al., 2017**), and SHALSTAB (**Marin et al., 2021b**), however, its capability to analyze the change of transient pore-water pressure provides good results in identifying landslide-susceptible areas (**König et al., 2021**).

An effort to predict landslide occurrences requires the knowledge of factors affecting the hillslope stability. Previous papers have discussed the landslide susceptibility of the West Bandung Regency region using the TRIGRS method approach (**Hermawan, 2023**). However, this study has not yet considered the effect of different rainfall intensities on shallow landslide susceptibility in the region. In this current study, we used the TRIGRS model to analyze the effect of rainfall intensity characteristics on shallow landslide susceptibility in the West Bandung Region. This study aims to (1) evaluate the parameters that affect slope stability, (2) determine the characteristics of rainfall that affect slope stability, and (3) assess the TRIGRS model performance to identify potential landslides triggered by rainfall. In this

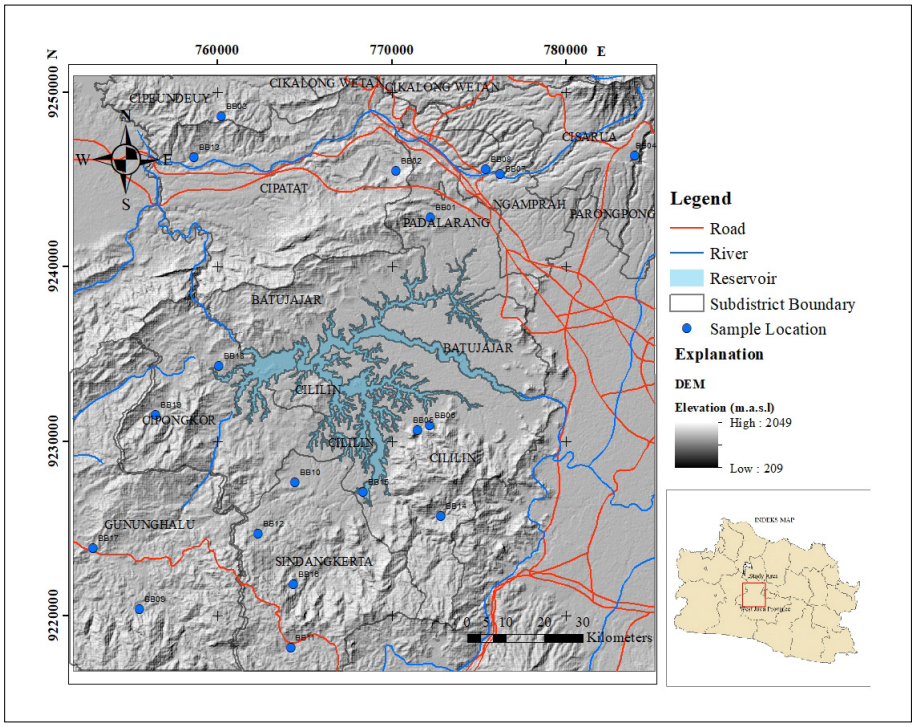

Figure 2: Research location.

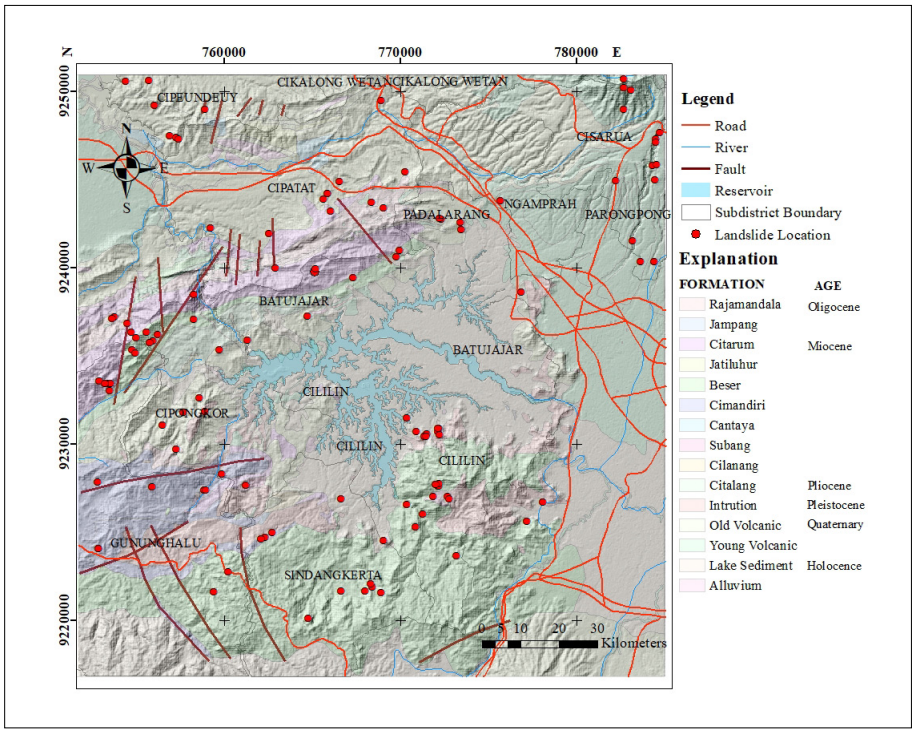

Figure 3: Geological map of the study area in West Bandung Regency.

study, the TRIGRS model is implemented to produce a landslide susceptibility map under the effect of the one-day antecedent rainfall intensity. The results of the initial condition model are compared with those of 6-hour and 12-hour rainfall models to determine rainfall characteristics triggering landslides. The receiver operating characteristics (ROC) analysis is used to evaluate the capabilities and effectiveness of the TRIGRS model in predicting areas prone to shallow landslides. Furthermore, the paper also thoroughly analyzes causative factors that influence landslide prediction in the study location.

2. Study Location Focus

2.1 Area general condition

The study area is located in the West Bandung Regency on the coordinates 9216779 – 9250979 N and

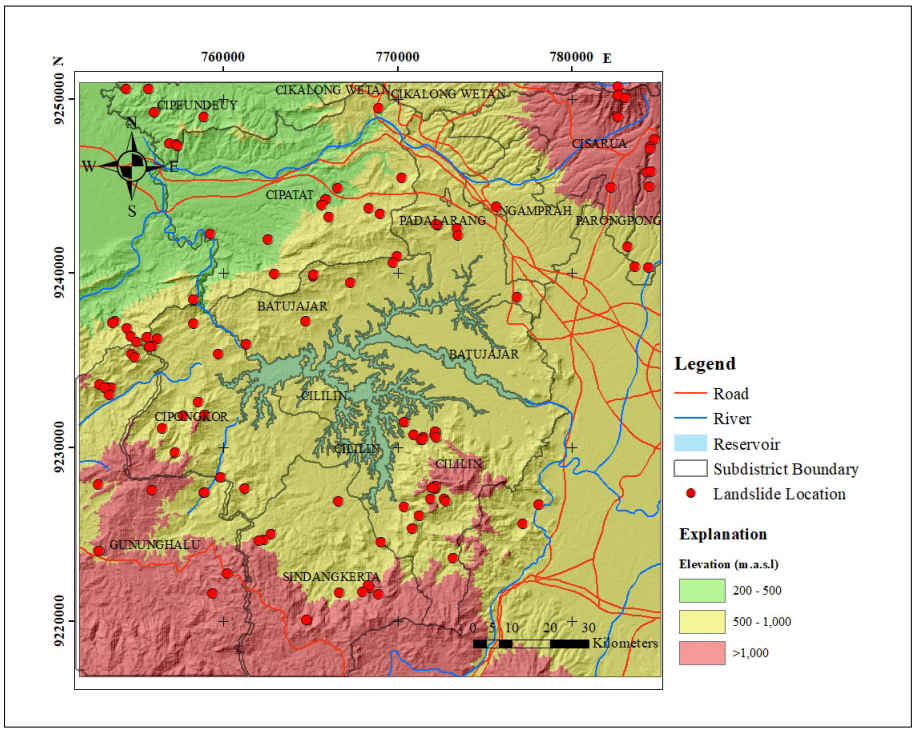

Figure 4: DEM raster map.

751683.7 – 785108.7 E in UTM 48 S Zone, on the west side of the Bandung basin, West Java Province, Indonesia (see **Figure 2**). This study area covers approximately 1,145 km^2. **Figure 2** shows the digital elevation model of the study area based on 1:25.000 digital maps produced by DEMNAS, Geospatial Information Agency, Indonesia (https://tanahair.indonesia.go.id/demnas/#/demnas). The highest elevation is 2,049 meters above sea level. According to **Figure 2**, the geomorphology of the study area mainly consists of hilly landscapes to high hills. This geomorphological condition contributes to the landslide susceptibility of the hilly landscape during the rainy season.

2.2 Geology of the research area

Based on the regional geological map shown in **Figure 3**, the study area stratigraphy is made up of rock formations ranging from old to young, namely the **Rajamandala** Formation of Oligocene – Early Miocene with lithological characteristics of clay, marl clay, marl, quartz sandstone, and conglomerate; the **Jampang** Formation composed of dacite tuff sandstone, pumice tuff, breccia, and tuffaceous clay (**Koesmono and Kusnama, 1996**); the **Citarum** Formation of Miocene age, characterized by breccia lithology, sandstone, siltstone; the **Jatiluhur** Formation of Early Miocene age with lithological characteristics of limestone, marl, quartz sandstone, basalt, and tuffaceous breccia; the **Beser** Formation of Early Miocene to Middle Miocene age, with tuffaceous breccia and lava lithology and andesite to basalt composition; the **Cimandiri** Formation of the older Middle Miocene composed of alternating claystone and light to medium gray siltstones, and yellowish-brown sandstones, locally calcareous, locally consisting of lava deposits composed of tuff, andesite breccias, and tuff breccias; the **Cantayan** Formation of Middle Miocene age with lithological characteristics of clay, marl, sandstone, limestone, shale, and breccia; the **Subang** Formation of Late Miocene, dominated by breccia, claystone, and sandstone lithology; the **Cilanang** Formation of Late Miocene with characteristics of the lithology of sandstone with molluscs, marl, limestone; the **Citalang** Formation of Pliocene age with lithology characteristics of tuffaceous marl, interspersed by tuffaceous sandstones and conglomerates (**Silitonga, 1973**); the Pleistocene **intrusion** of hornblende andesite, pyroxene andesite, and andesite; Quaternary **Old Volcanic** deposits characterized by breccia lithology, lahars, and layered tuff sandstone with a gentle slope; and Quaternary **Young Volcanic** deposits with lithology characteristics in the form of tuffaceous sandstone, lapilli, tuffaceous breccia, lava, and agglomerates originating from Mount Tangkubanparahu and Mount Tampomas.

Other rock formations of the fluvial depositional environment are also present in the study area, namely, Holocene **Lake Deposits** composed of lithology silt, clay, fine sand, coarse sand, gravel, and tuffaceous conglomerates; and Holocene **Alluvium** consisting of silt, clay, fine sand, coarse sand, and gravel sand as well as chunks of igneous and sedimentary rocks.

The regional geological structure developed in this study location is characterized by folds and faults (**Sudjatmiko, 1972**). They consist of the Cipongkor syncline, the normal fault in the Cipatat area of the Rajamandala Formation Citarum Formation and Beser Formation, and the strike-slip fault in the Cipeundeuy area of the Ja-

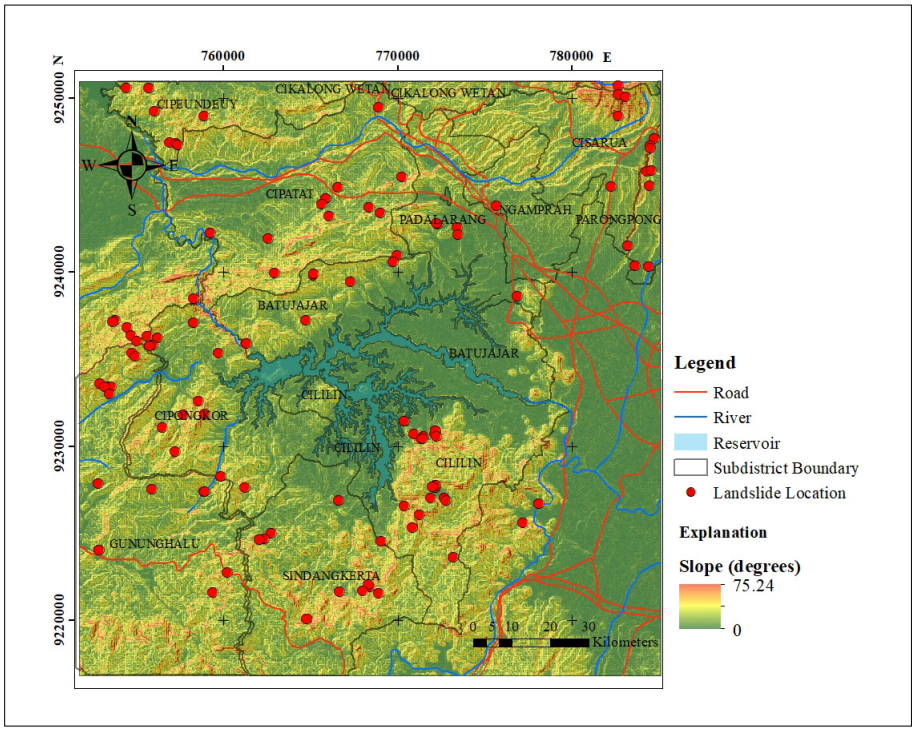

Figure 5: Raster map of the slope angles and occurrences of landslide.

tiluhur Formation, the Cantayan Formation and the Old Volcanic. Meanwhile, **Bronto and Langi (2016)** stated that the Cimandiri Fault is trending southwest-southwest-northeast of the Cimandiri Formation. The geological map of the research area represents several landslide distributions in the area of volcanic geological units dominated by breccia, tuff, and tuffaceous breccia units, as well as several landslide locations in the regions that are developing geological structures.

3. Research Material and Methods

3.1 Topographic slope

For the analysis of digital topographic maps, input data for topographic slope parameters are acquired from DEMNAS with a scale of 1:25,000. The digital elevation model (DEM) of the study area was created using the GIS software. The DEM was divided into grids of 25 m×25 m (see **Figure 4**). Data sets of local landslide inventory were collected from field surveys, visual identification from Google Earth, and the database of the Center for Volcanology and Geological Hazard Mitigation, Indonesia, with a total of 113 landslide events. The study area is mainly located at the elevation of 500-1,000 meters above sea level around 64.3% of the total area. The landslide event in this study is approximately 70.8% distributed in that elevation (see **Figure 4**, shown in yellow).

The DEM is then used to generate raster maps of flow direction and slope. The DEM is also used to produce the slope gradient distribution of each cell. **Figure 5** depicts the characteristics of a hilly morphology mainly consisting of hilly landscapes to high hills in the north-

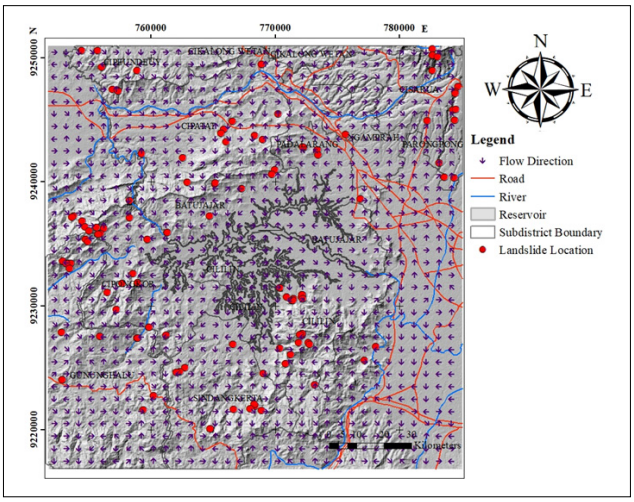

Figure 6: Flow direction raster map and landslide locations.

east and southwest. Besides, the transformation from flat to hilly area is well seen in the central areas to the east. As indicated in **Figure 5**, the history of landslide events is prevalent in hilly areas with moderate to steep slopes with slope angles ranging from 21% to 54%. Thus, slope angles significantly contribute to landslide occurrences in the study area. In implementing runoff routing calculations, it is necessary to know the direction of the downslope cells that limit the steepest in correspondence with each cell in the TRIGRS model.

The research location was dominated by the northward flow direction covering an area of 226 km^2 to the Cipatat, Cililin, and Gununghalu area, the westward flow direction covering an area of 223 km^2 to the Cililin, Cipatat, Padalarang, and Cisarua area, and the south-

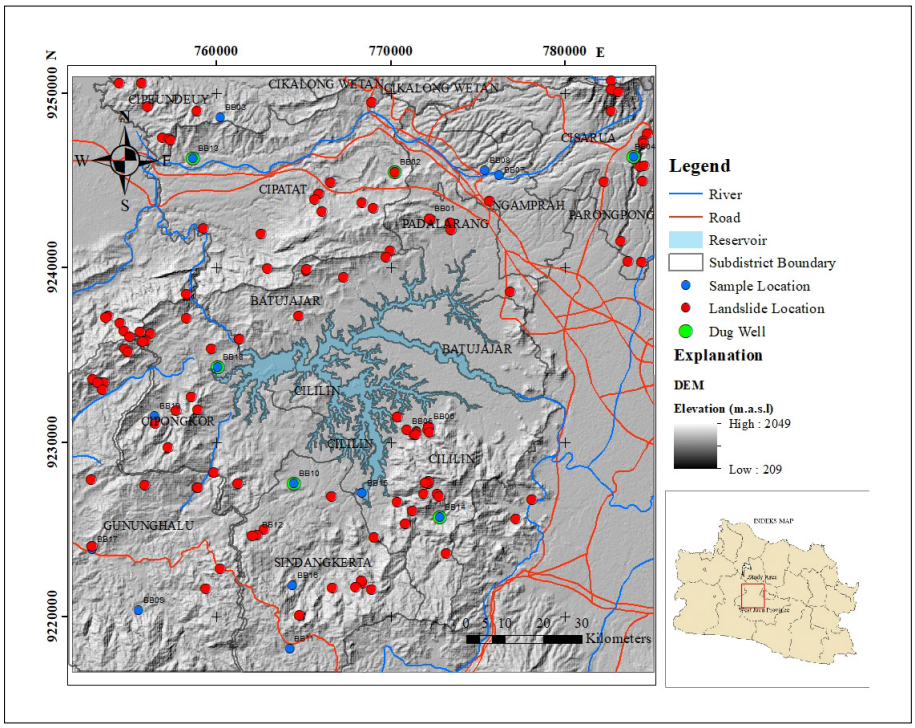

Figure 7: Soil sampling location map.

Table 1: The results of laboratory tests for soil engineering properties.

Code	Location	Effective cohesion c' (Pa)	Unit weight (N/m³)	Effective friction angle phi' (θ)	Porosity (n)	Saturated hydraulic conductivity, Ks (m/s)	Infiltration rate (m/s)	Hydraulic diffusivity, D_0 (m/s)
BB01	Padalarang	17370.78	16628.36	12.65	0.56	1.62E-06	2.65E-03	2.65E-05
BB02	Cipatat	2640.54	15882.46	18.84	0.62	2.44E-06	5.12E-02	5.12E-04
BB03	Cipeudeuy	4044.97	16114.13	16.38	0.56	9.32E-06	6.78E-03	6.78E-05
BB04	Cisarua	4317.27	12329.34	14.24	0.62	1.26E-05	3.67E-02	3.67E-04
BB05	Cililin	3865.42	15569.39	13.83	0.57	8.21E-10	4.45E-03	4.45E-05
BB06	Cililin	2729.40	17335.78	29.71	0.49	8.97E-06	5.45E-02	5.45E-04
BB07	Ngamprah	3420.47	14461.80	28.75	0.60	5.34E-09	9.46E-03	9.46E-05
BB08	Ngamprah	4539.31	17176.73	20.27	0.52	3.13E-05	4.11E-03	4.11E-05
BB09	Gunung Halu	16553.06	16790.19	28.88	0.51	2.85E-09	2.40E-03	2.40E-05
BB10	Sindangkerta	17545.16	12890.96	26.87	0.62	2.60E-05	2.82E-03	2.82E-05
BB11	Sindangkerta	9996.51	12833.67	23.70	0.63	1.74E-06	1.98E-02	1.98E-04
BB12	Sindangkerta	17174.49	16114.39	24.08	0.56	4.06E-09	3.84E-03	3.84E-05
BB13	Cipatat	21578.79	11581.24	15.19	0.68	1.39E-09	1.54E-03	1.54E-05
BB14	Cililin	2641.09	21069.39	23.58	0.51	4.48E-10	7.47E-04	7.47E-06
BB15	Cililin	21422.60	9674.00	14.54	0.77	1.13E-06	2.47E-02	2.47E-04
BB16	Sindangkerta	1669.56	16541.11	24.52	0.51	1.58E-09	4.88E-03	4.88E-05
BB17	Rongga	9197.57	16482.79	29.90	0.54	8.78E-09	1.47E-02	1.47E-04
BB18	Cipongkor	2021.81	16515.44	22.21	0.50	4.79E-10	8.90E-03	8.90E-05
BB19	Cipongkor	9609.26	14313.04	26.04	0.58	9.50E-06	3.78E-02	3.78E-04

ward flow covering an area of 189 km² to the Padalarang, Ngamrah, Parompong, and Batujajar area, and the eastward flow direction covering an area of 172 km² up to the Gununghalu, Cililin, and Sindangkerta area. The landslide distribution is located in eight directions: north (22% of events), south (19% of events), west (16% of events), east (19% of events), northwest (10% of events), southeast (19% of events), southwest (19% of events), and northeast (19% of events) shown by an arrow (see **Figure 6**).

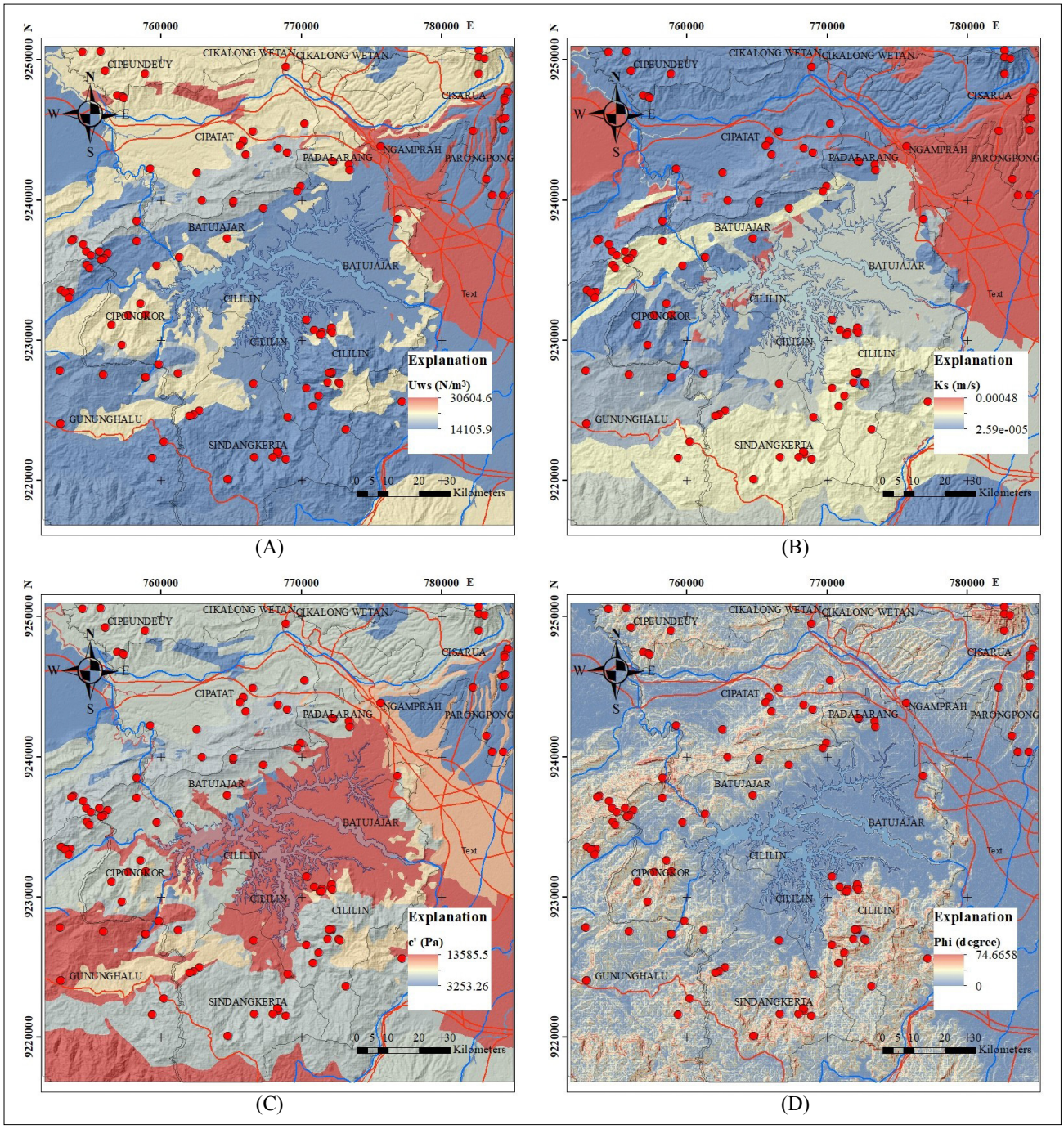

Figure 8: The landslide occurrences distribution on soil engineering properties map; (A) unit weight, (B) saturated hydraulic conductivity, (C) effective cohesion, and (D) effective friction angle.

3.2 Soil engineering properties

In this research, undisturbed soil samples were taken from several locations representing different geological units using a soil sampler (see **Figure 7**) to obtain physical and engineering soil properties required for the infiltration process and slope stability calculation in the TRIGRS model. Laboratory tests include soil unit weight (γ_w) test and shear strength test. Shear strength parameters, the effective soil cohesion (c'), and the effective shear angle (φ') were obtained from triaxial compression tests in consolidated undrained conditions. The saturated hydraulic conductivity coefficient (Ks) was determined using the falling head permeameter tested. **Table 1** shows the summarized soil properties for each geological unit.

TRIGRS modelling also requires input parameters related to soil hydraulic diffusivity. Soil hydraulic diffusivity, D_0, was determined as the correlation of the coefficients of saturated hydraulic conductivity (Ks), where

previous studies found approximately 10-500 times the hydraulic conductivity value in colluvium soil (**Park et al., 2013**). This study assumes that 100 times the *Ks* value (**Baum et al., 2005**) given by:

$$D_0 = 100 \text{ x } K_s \quad (1)$$

Figure 8 presents maps of soil engineering properties overlayed with landslide location distributions obtained based on **Table 1**. Because the soil properties data are rare for each rock formation, the spatial join analysis tool available in GIS software was used to create a map of soil engineering properties using **Table 1**. This analytical method was also used in the study of regional rainfall-induced slope failures in Malaysia (**Saadatkhah et al., 2015**). A raster map of soil engineering properties was created using the polygon to raster GIS conversion tool for all value parameters for each geological unit. **Figure 8A** presents the distribution of landslide occurrence in the soil unit weight map. Most of the landslide occurrences are located in hilly areas of low soil unit weight. In **Figure 8B,** the landslide incidents are dominantly distributed in hilly areas with low saturated hydraulic conductivity coefficients. Low hydraulic conductivity indicates the slope surface capability to pass water at a prolonged flow rate in these areas. So, when the hydraulic conductivity of the soil is poorer, the water is retained longer, and the soil becomes more saturated. Soil saturation can occur when there has been a lot of rain for a long time (**Hong et al., 2018; Huang and Lin, 2002**). Saturation causes an increase in the pressure of pore water and eventually causes a decrease in the strength of soil shear, consequently triggering susceptibility landslides. It is evident in **Figure 8C** and **Figure 8D** that most landslide occurrences are mainly in hilly areas with low soil cohesion and friction angles. In other words, the hilly areas with low soil shear strength are very prone to rainfall-induced landslides.

3.3 Soil Thickness

Morphology and relief are factors that influence the formation process of soil thickness. In areas with high elevations or in the hills, the soil layer is thinner due to erosion, whereas a thicker soil layer is formed due to the sedimentation process in flat areas. So, for the effective soil thickness parameter, it is assumed spatially using the linear equation function of the elevation. The soil thickness is also an essential parameter in the TRIGRS model (**Baum et al., 2002**). Soil thickness affects infiltration and soil cohesion in deterministic shallow landslide models.

Mapping soil thickness is complex, costly, and time-consuming. Several methods of spatial interpolation are applied to mapping various soil thicknesses using the function of terrain attributes: elevation (**Saulnier et al., 1997**), slope inclination (**Schilirò et al., 2018**), and slope curvature (**Montgomery and Dietrich, 1994**; **Mehnatkesh et al., 2013**). Field soil depth observations and the topographic factors derived from DEM produced good soil depth correlation. Thus, this study used a simple relationship that assumes the soil thickness associated with the elevation derived from the DEM map. In this study, the soil depth uses a linear drop elevation function to map spatially (**Saulnier et al., 1997**), expressed as:

$$m_i = m_{max} - (m_{max} - m_{min}/z_{max} - z_{min}) \text{ x } (z_i - z_{min})) \quad (2)$$

Where:

m_{min} – the minimum effective soil thickness (m),
m_{max} – the maximum effective soil thickness in a cell (m),
z_i – the elevation at point i in a cell (m),
z_{min} and z_{max} – the minimum and maximum elevation at a cell, respectively (m).

The distribution of soil thickness is shown in **Figure 9**. The values of the minimum and the maximum soil thickness are 0.05 m and 7.0 m, respectively. **Figure 9** indicates landslide occurrences are mainly located in hilly areas with a soil layer of 0.58 to 6.85 m thick. As a result, landslides are restricted to hilly areas with soil thicknesses less than 7.0 m in this area.

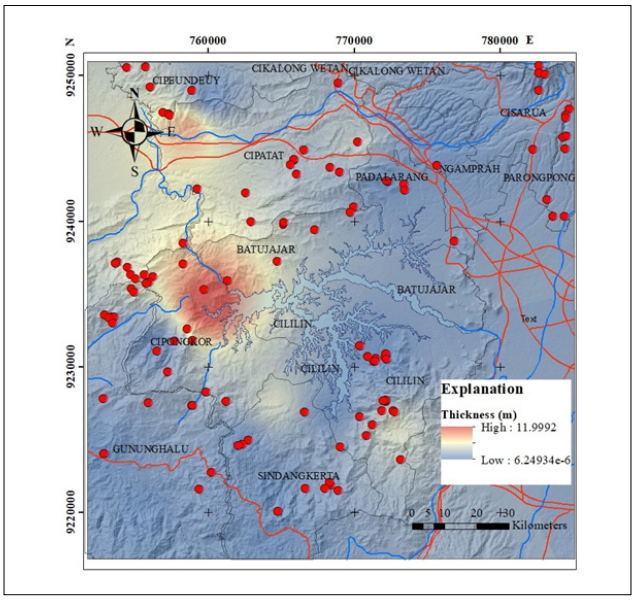

Figure 9: Distribution of landslide occurrences against soil layer thickness.

3.4 Groundwater table

Shallow slope failure occurrences are mainly due to rising groundwater tables and pore water pressure. So, the groundwater table is one of the hillslope stability controlling parameters. In this study area, the measurement of groundwater depth conducted in 6 dug wells at landslide locations indicates that a shallow groundwater level was of about 1 to 4 m with an average depth of 2.5 m present in the study area (see **Figure 7**). Therefore, based on TRIGRS' ability to predict the occurrence of shallow slides with slip planes near the surface slopes,

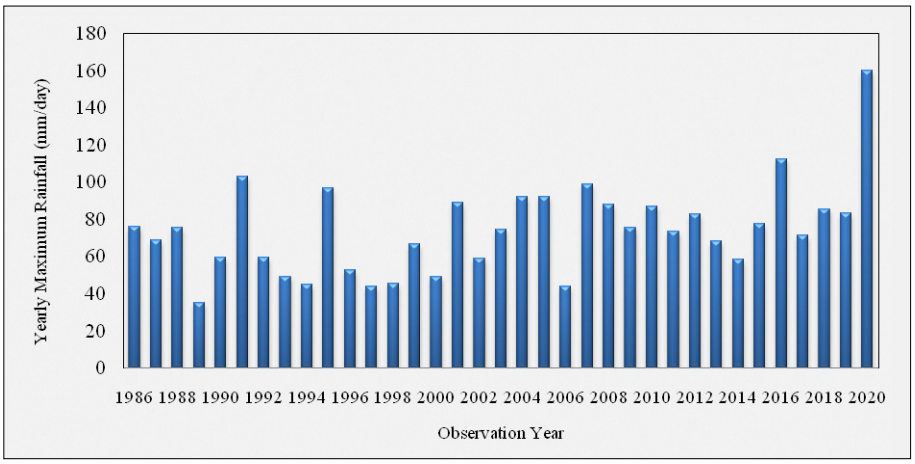

Figure 10: Daily maximum rainfall intensity graph (mm/day) 1986 – 2020.

this study applied an average groundwater depth of 2.5 m in the TRIGRS modelling.

3.5 Rain intensity and return period

Rainfall data for this study was collected over 35 years from several meteorological stations distributed in the study area. Based on the collected rainfall data, the daily maximum rainfall data were determined (see **Figure 10**) and then analyzed using the Gumbel distribution theory to obtain probability and rainfall distribution curves (see **Figure 11**).

As mentioned previously, there has been an increase in landslide occurrences in the study area during the last ten years. According to **Figure 11**, the rainfall for a 10-year return period is 111 mm/day, with a probability of around 68%. Two scenarios of rainfall intensity and duration were considered for the susceptibility modelling to evaluate the influence of different rainfall characteristics on landslide susceptibility in the study area. Scenario A considered a short period of rainfall, which was assumed to last for 6 hours in one day prior to the landslide. In scenario B, a long period of rainfall was considered to last for 12 hours one day prior to the landslide incident. Long-duration rainfall causes fewer antecedent rainfall-induced landslides (**Huang and Lin, 2002**). The rainfall intensity for short and long-period scenarios was determined using Mononobe's formula (**Fang and Chen, 1995**) as shown in **Equation 3**, as follows:

$$I = \frac{R_{24}}{24} \times \frac{24^{\left(\frac{2}{3}\right)}}{t} \quad (3)$$

Where:

I – the rain intensity plan (in mm/hour),

R_{24} – the daily maximum rainfall in 24 hours (in mm/day),

t – rain duration (in an hour).

Table 2 shows rainfall intensity and duration determined using Mononobe's formula for each scenario used in the TRIGRS model. For scenario A, a short period of heavy rain of 6 hours was characterized by a rainfall intensity of 11.65 mm/hour. Meanwhile, the rainfall intensity of 7.43 mm/hour for 12 hours represents the long period of light rain in scenario B.

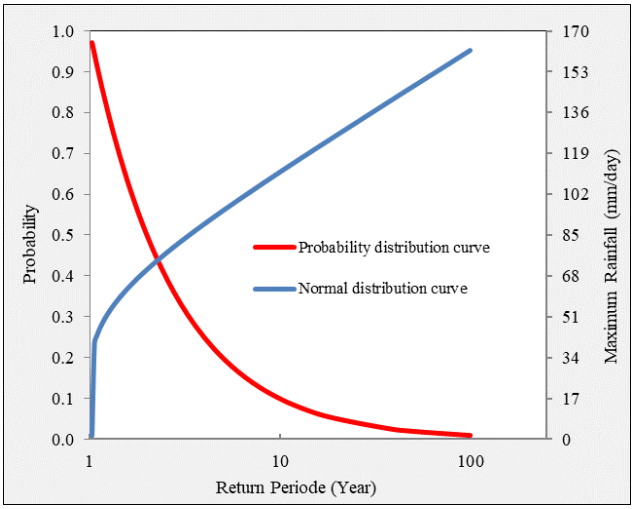

Figure 11: Gumbel's method of the probability distribution curve.

Table 2: Rainfall intensity scenarios used in the landslide susceptibility modelling.

Scenario	Rainfall intensity (mm/hour)	Duration (hour)
A	11.65	6
B	7.34	12

3.6 The TRIGRS Model

The USGS developed a Transient Rainfall Infiltration and Grid-based Regional Slope-Stability Analysis. The model is called TRIGRS. This model was applied to analyze rainfall-induced landslides in this study (**Baum et al., 2002**). TRIGRS is a model used to compute slope stability using analytical solutions to calculate the safety factor value to transient pore water pressure using an infinite slope analysis approach to rainfall-induced (**Baum**

Table 3: Input parameters for the TRIGRS model in this study.

Parameter	Unit	Attributed Value	Source
Slope angle *(δ)*	(°)	Spatially varies	25 x 25 m DEM
Soil thickness *(Zmax)*	(m)	Spatially varies	Elevation function (**Saulnier et al., 1997**)
Friction angle *(φ')*	(°)	Spatially varies	Soil triaxial test
Cohesion *(c')*	(Pa)	Spatially varies	Soil triaxial test
Soil unit weight *(γ_s)*	(N/m^3)	Spatially varies	Soil triaxial test
Hydraulic conductivity *(K_z)*	(m/s)	Spatially varies	Infiltration test
Hydraulic diffusivity *(D_0)*	(m^2/s)	Spatially varies	100 x *Ks* (**Baum et al., 2005**)
Initial depth of water table *(d)*	(m)	2.5	Assumption
Initial rainfall *(I_{ZLT})*	(m/s)	0	Steady-state
Rainfall rate *(I_z)*	(mm/h)	Spatially constant	BMKG & PLTA

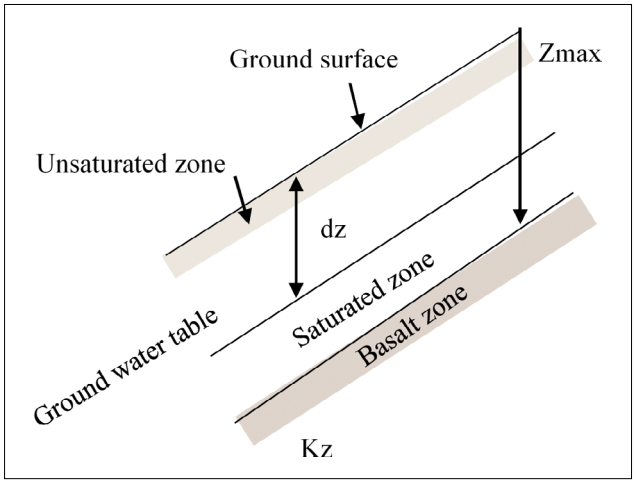

Figure 12: Illustration of slope conditions in the TRIGRS model concept (from **Baum et al., 2002; Baum et al., 2010**).

et al., 2002; Baum et al., 2010). This model was designed using the FORTRAN programming language. TRIGRS is crucial for mapping landslide occurrence, prevention, and investigations. TRIGRS can be used as a land-use design for regional areas against landslide hazards. TRIGRS requires input parameters, i.e. soil hydraulic condition, parameters of shear strength soil, and rainfall infiltration. Except for the rainfall rate parameter, input parameters for this TRIGRS modelling in this study vary spatially (see **Table 3**).

The infiltration in the TRIGRS model applied a linear principle (**Iverson, 2000**) and an extension of Richard's formula. Iverson's infiltration formula consists of steady and transient conditions. A steady state is a condition at the initial filtration input rate and the inclination angle where the flow is in an unbalanced direction (**Iverson, 2000**). Transient infiltration is a condition that considers the flow of vertical downward, the surface flux of varying time series for variable intensity and duration, and the condition of zero-flux at times more than the early border of infinitely deep basal (see **Figure 12**).

The following formula gave the pore pressure for layers saturated of the basal zone with ψ as the groundwater pressure head at depth Z and time t. Z originates $z/\cos\delta$ where Z is positive in the downward direction and depth below the ground surface; δ is the slope angle; z is normal to the slope angle and the t parameter is the time. d is the steady-state depth of the water table measured in the vertical direction, d_{LZ} is the saturated layer depth in the basal zone measured vertically, $\beta = \cos^2\delta - (I_{ZLT}/Ks)$, Ks is the saturated hydraulic conductivity in the Z direction, I_{ZLT} is the steady surface flow, I_{nZ} as the surface flow of a given intensity for the nth time interval. Further, $D1$ originates $D0/\cos^2\delta$, the saturated hydraulic diffusivity $(D0) = Ks/Ss$, the saturated hydraulic conductivity (Ks), and the specific storage (Ss). N is the total number of time intervals; $H(t-tn)$ is the Heaviside step function, and tn is the time at the nth time interval in the rainfall infiltration sequence; erfc(η) is the complementary error function: ierfc(η) = $(1/\sqrt{\pi})\exp(-\eta^2) - \eta\,\mathrm{erfc}(\eta)$ m is the index of infinite series displaying an odd term in the complementary error function, given by **Baum et al. 2002**:

$$\psi(Z,t) = [Z-d]\beta$$

$$+2\sum_{n-1}^{N}\frac{I_{nz}}{K_s}H(t-t_n)\left[D1(t-t_n)\right]^{\frac{1}{2}}\sum_{m=1}^{\infty}\left\{\begin{array}{l} ierfc\left[\dfrac{(2m-1)d_{LZ}-Z}{2\left[D_1(t-t_n)\right]^{\frac{1}{2}}}\right] \\ +ierfc\left[\dfrac{(2m-1)d_{LZ}+(d_{LZ}-Z)}{2\left[D_1(t-t_n)\right]^{\frac{1}{2}}}\right]\end{array}\right\}-$$

$$+2\sum_{n=1}^{N}\frac{I_{nz}}{K_s}H(t-t_{n+1})\left[D1(t-t_{n+1})\right]^{1/2}\sum_{m=1}^{\infty}\left\{\begin{array}{l} ierfc\left[\dfrac{(2m-1)d_{LZ}-Z}{2\left[D_1(t-t_{n+1})\right]^{\frac{1}{2}}}\right] \\ +ierfc\left[\dfrac{(2m-1)d_{LZ}+(d_{LZ}-Z)}{2\left[D_1(t-t_{n+1})\right]^{\frac{1}{2}}}\right]\end{array}\right\} \quad (4)$$

In this model study, the safety factor (SF) calculation uses an analytical formula to analyze the failure of an infinite slope, described as the ratio of the resistive force to the driving force on the slope. A safety factor formula of an infinite slope in the model uses parameters including φ' as the effective friction angle of the soil and c' as the effective soil cohesion. Further, ψ (Z,t) is the pres-

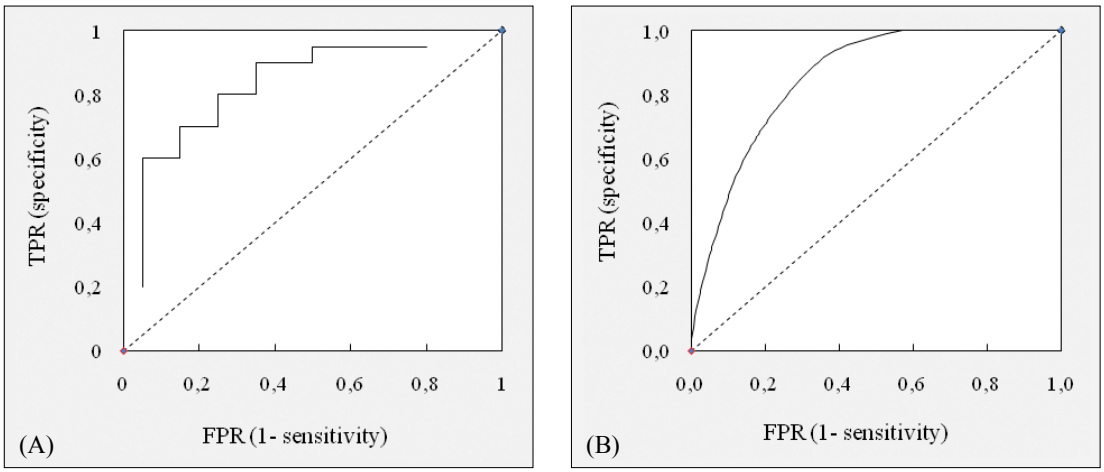

Figure 13. ROC curve (A) discrete and (B) continuous case (modified **Gorunescu, 2011**).

Table 4: Performance classification (**Gorunescu, 2011**).

AUC index values	Classification
0.9 - 1.0	Very Good
0.8 - 0.9	Good
0.7 - 0.8	Fairly Good
0.6 - 0.7	Bad
0.5 - 0.6	Incorrect

sure head in the saturated zone at depth Z and time t, γ_s is the unit weight, γ_w is the unit weight of water, and θ is the sliding plane angle for each grid cell given by (**Iverson, 2000**):

$$SF = \frac{c' - \psi(Z,t)\gamma_w \tan\phi'}{\gamma_S Z \sin\theta\cos\theta} + \frac{\tan\phi'}{\tan\theta'} \quad (5)$$

The slope safety factor is controlled by the strength of resistance and stress shear acting in the slip plane. A safety factor is a value that states the condition of slope stability abbreviated with the SF value. The slope is stable on the condition that an SF value of more than 1.0; otherwise if it has an SF value less than 1.0, it is unstable. **Equations** (**4**) and (**5**) are combinations of the value of the safety factor spatial distribution calculated based on rainfall and parameter input data.

Soil engineering properties were determined from laboratory tests on undisturbed samples from different geological units that formed raster with cell pixels 25x25 m.

3.7 ROC (Receiver Operating Characteristic) curve

In modelling, a method to illustrate the classification model performance of all classification thresholds uses analysis of the receiver operating characteristic curve (ROC). The ROC curve is a method to visualize, organize, and select the classifier based on model performance (**Fawcett, 2006**). ROC is a two-dimensional graph with the proportion of false positives (specificity) as the prediction rate on the horizontal axis and the proportion of true positives (sensitivity) as the success rate on the vertical axis (see **Figure 13).** In this respect, the ROC curve as an independent threshold method is used to evaluate the influence of the causal factor parameters on landslides (threshold-independent method) (**Chung and Fabbri, 2003**). The ROC forms part of the unit square area whose value is between 0 and 1.0, called AUC or Area Under Curve. In other words, the AUC is an area under the ROC curve to measure an ability model classifier. The AUC value is one type of statistical accuracy for predictive (probability) models in natural disaster assessment analysis. Evaluation of model performance accuracy based on the AUC value of the ROC curve can be classified into five groups (see **Table 4**). In this study, the ROC curve analysis was conducted to evaluate the level of significance of each parameter in controlling the landslide susceptibility of the TRIGRS modelling results.

The AUC calculation formula used in this study by **Beguería** (**2006**) is as follows:

$$\mathrm{AUC} = \sum_{i=0}^{n} (x_i - x_{i-1}) y_i - \left[\frac{(x_i - x_{i-1})(y_i - y_{i-2})}{2} \right] \quad (6)$$

Where:

x_i – the proportion of landslide area (%)

y_i – the proportion of landslide events (%).

4. Results and Discussion

4.1 Effect of rainfall on spatial and temporal slope stability

Figure 14 shows the results of the TRIGRS model for the initial condition for scenarios A and B, which indicates the hillslopes in the study area are in a dominantly stable condition (SF > 1.0). The unstable hill slope (SF < 1.0) was dominantly distributed only in the northeastern part of the study area as indicated by a blue circle, characterized by steep to very steep slopes and thin soil thickness. Thus, factors such as slope angles and soil thickness are

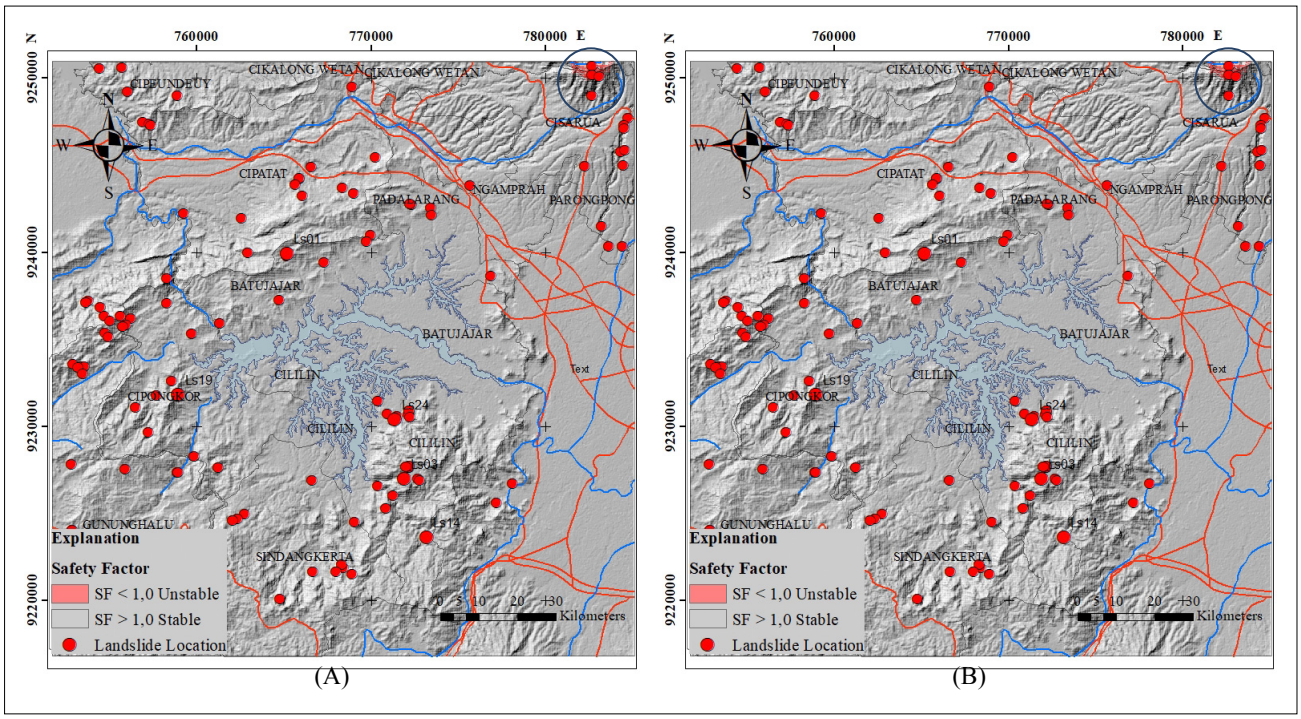

Figure 14: TRIGRS modelling results at initial condition scenario A (A) and scenario B (B).

the most controlling parameters for hillslope stability in this study. In several landslide susceptibility studies, the slope angle is one of the controlling parameters for the shear forces acting on hill slopes (**Nefeslioglu and Gokceoglu, 2011; Lepore et al., 2012**).

The results of slope stability modelling for each scenario, represented in **Figure 15** and **Figure 16,** show that the unstable hillslope areas increase significantly in both scenarios at the end of the rainfall period. This proves that any rainfall intensity of a given duration affects the stability of hillslopes in the study area, especially on moderate-to-steep hillslopes. The modelling results also revealed that steep hillslope areas with high stability remain stable for both scenarios. Referring to **Figure 8**, the cohesion and friction angles of the steep hillslopes are significantly high. This modelling result demonstrates that rainfall infiltration could not reduce the stability of steep hillslopes made up of soil layers of higher shear strength. In other words, soil shear strength plays an important role in maintaining the stability of steep hillslopes during a rainfall period.

4.2 Effect of rainfall characteristics on landslide susceptibility

Based on the results of the TRIGRS modelling, the histogram graph shows a decrease in the stable slopes area and an increase in the unstable slopes area from the first hour to the last hour. **Figure 17** and **Figure 18** show the expansion of the unstable slope area by approximately 11.5% in scenario A and 16.4% in scenario B. These results implied that the rainfall intensity can affect the stability of the hillslope, from stable to unstable conditions, as indicated by a decrease in the slope safety factor (SF) value, hence, the hillslope is prone to landslides.

Based on the comparison, the modelling result shows that the influence of the one-day antecedent rainfall was perceived in two scenarios, i.e. 6 hours and 12 hours. **Figure 19** shows that a long period of antecedent rainfall affects the hillslope stability more significantly than a short period of rainfall in the study area. Based on this figure, it is very obvious that rainfall of long duration makes the slopes more unstable (scenario B) because rainwater that infiltrates into the slopes is retained longer, and hence, the slopes become more saturated than short durations (scenario A). Therefore, the duration of rainfall has a more significant impact on slope stability than rainfall intensity.

4.3 Relationship between landslide susceptibility and geological conditions

The relationships between the landslide inventory data and the TRIGRS modelling results for every rock formation are shown in **Figures 20** and **Figure 21.** Based on these figures, events mainly occurred in the Beser Formation which is dominantly composed of volcanic rocks. The TRIGRS modelling also shows the unstable hillslope mainly concentrated in the Beser Formation. Thus, the TRIGRS modelling results have a good correlation with the landslide inventory data.

The TRIGRS modelling results demonstrate that the landslide susceptible areas increase with rainfall duration in both scenarios. In scenario A, the unstable hillslope areas cover up to 63.67 km^2 in the Beser Formation, 20.68 km^2 in the Citalang Formation, and 11.22

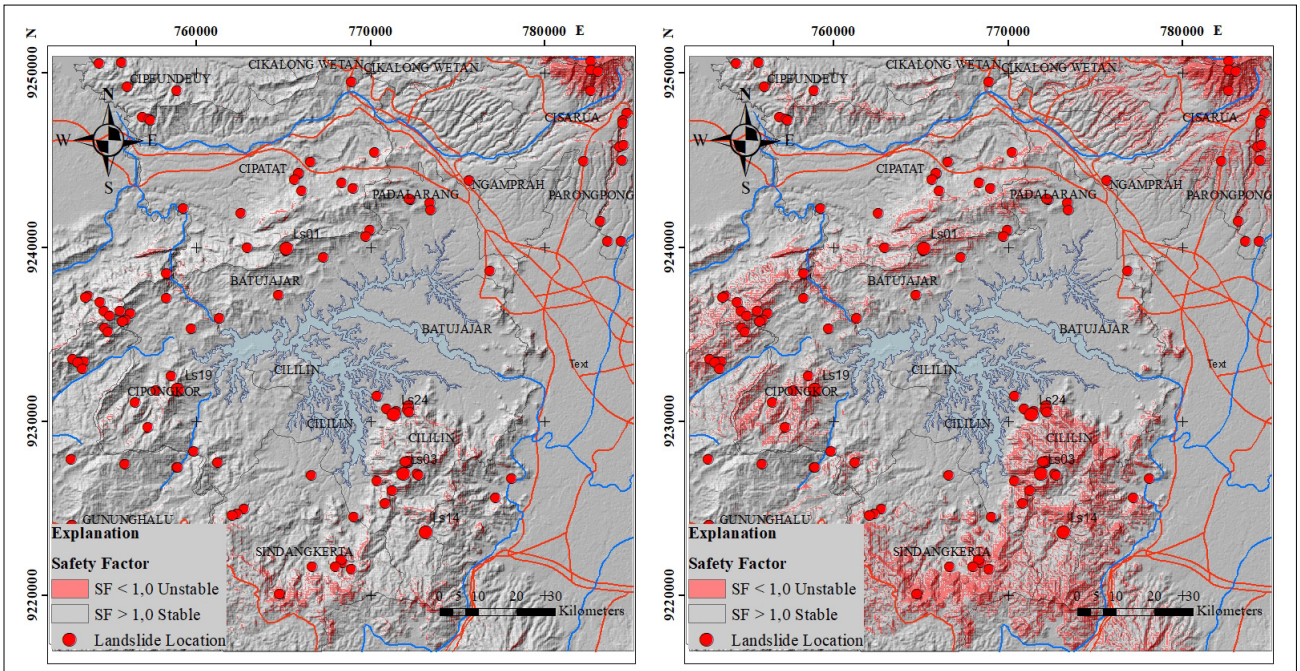

(A) 3 hours-rainfall (B) 6 hours-rainfall

Figure 15: TRIGRS modelling results in scenario A for the 6-hour duration (A) the first 3 hours and (B) 6 hours.

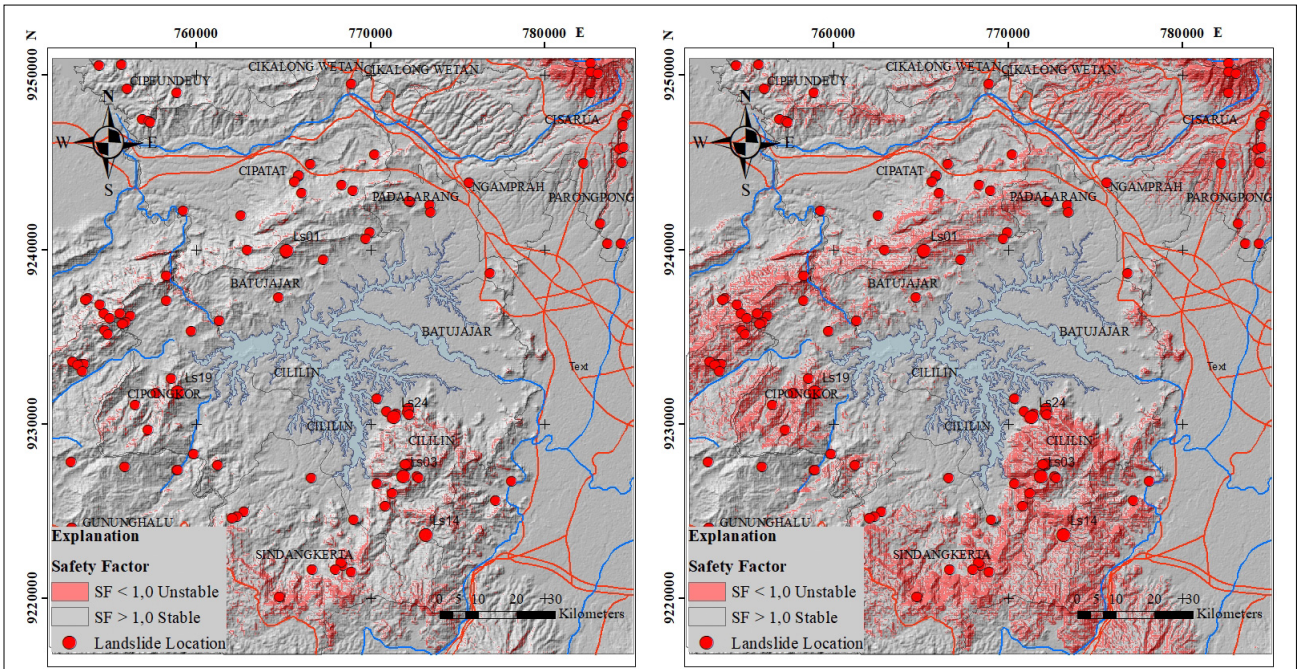

(A) 4 hours-rainfall (B) 12 hours-rainfall

Figure 16: TRIGRS modelling results in scenario B for the 12-hour duration (A) the first 4 hours and (B) 12 hours.

km² in the Citarum Formation when the rainfall period ends (see **Figure 20**). Similarly, the landslide-susceptible areas in scenario B increase from T0 to T12, reaching up to 80.97 km² in the Beser Formation, 49.18 km² in the Citalang Formation, and 19.23 km² in the Citarum Formation (see **Figure 21**). Thus, according to the modelling results, the rock formation also affects the landslide susceptibility in the study area. In all rainfall scenarios, the Beser rock formation is more prone to landslides than other rock formations, and its susceptibility increases more significantly under the increase in rainfall duration. In other words, rainfall duration has a more pronounced effect than rainfall intensity on landslide susceptibility in the study area.

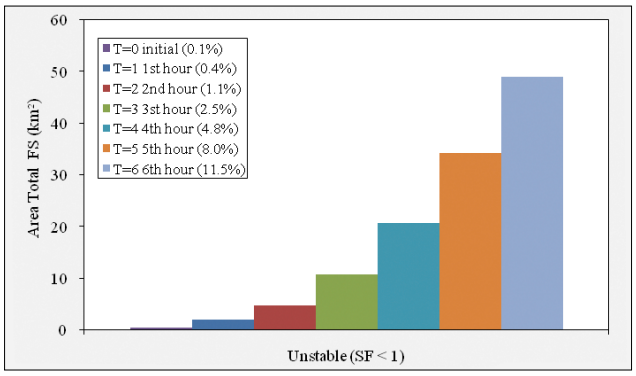

Figure 17: The area of stable and unstable slopes in scenario A.

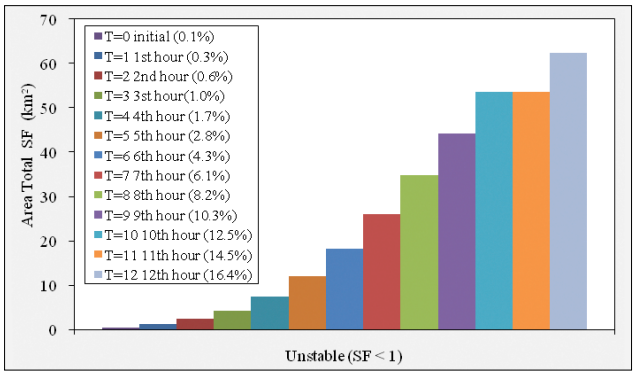

Figure 18: The area of stable and unstable slopes in scenario B.

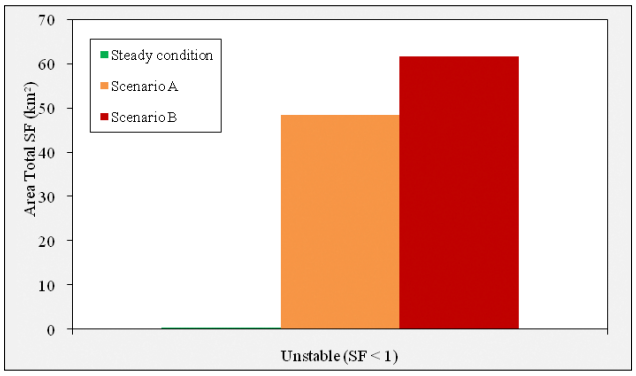

Figure 19: Comparison of the area of unstable slopes in scenarios A and B.

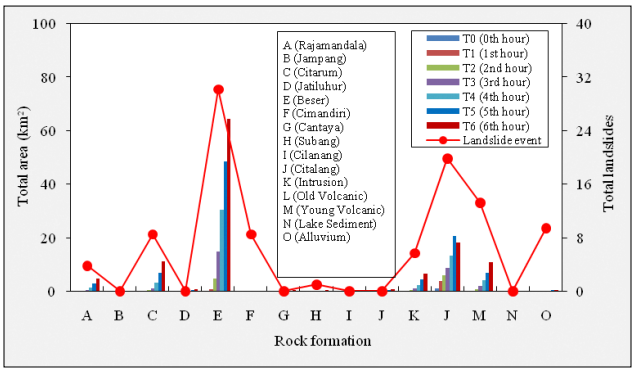

Figure 20: The total unstable area in each rock formation in scenario A.

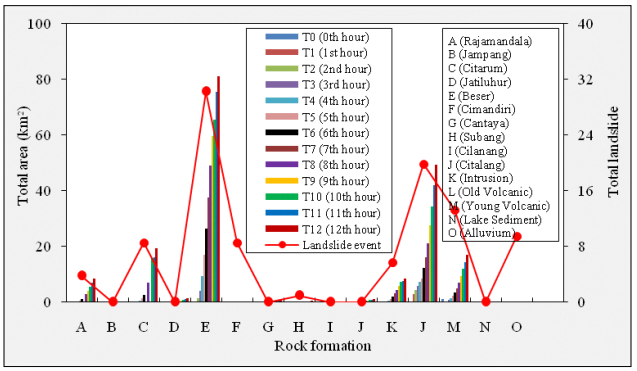

Figure 21: The total unstable area in each rock formation in scenario B.

Figure 22 shows the distribution of unstable hillslopes in areas that have developed geological structures. From this figure, it can be seen that some historical landslide events were distributed in the areas of high lineament density. Thus, the geological structure can be one of the controlling factors of landslide susceptibility because it is associated with the weathering process of the rock, by which the rock becomes more permeable. Consequently, the rainwater can infiltrate the rock through the weathered weak zone. The distribution of unstable hillslopes is also found in steep hilly areas without geological structure in the Cililin and Sinandgkerta areas (shown in the blue rectangle). These areas are geologically made up of volcanic rocks (see **Figure 3**). Referring to **Figure 3** and **Figure 8,** the hillslopes of the Beser Formation are very prone to landslides because the soils have low shear strength. Thus, the hilly areas without any geological structure influences, soil shear strength will control the susceptibility of the areas to landslides.

Other soil property parameters, such as hydraulic conductivity (*Ks*) and unit weight of soils (g*s*) also have a significant control on the hillslope susceptibility to landslide. Referring to unit weight and hydraulic conductivity maps (see **Figure 8A** and **Figure 8B**) and the TRIGRS modelling result (see **Figure 16B**), hillslopes with low to medium *Ks* and g_s are more susceptible to landslides than those with high *Ks* and g_s. Low soil coefficients of hydraulic conductivity cause the soil to retain the rainwater for a long time, resulting in the saturation of the soil layer during a rainfall period. Thus, infiltration of rainwater into low hydraulic conductivity soils is more sensitive to rainfall duration than to rainfall intensity (**Aristizábal et al., 2020**). Similarly, hillslopes with a low soil unit weight are also more prone to landslides because the hillslopes are made up of clay-rich soils of low hydraulic conductivity that will control the soil saturation as explained previously. Thus, it is clear that the physical and mechanical properties of soils may influence the landslide occurrences in the study area. Some previous studies (**Mugagga et al., 2011**; **Zung et al., 2009**) also indicated that the stability of any hillslope is

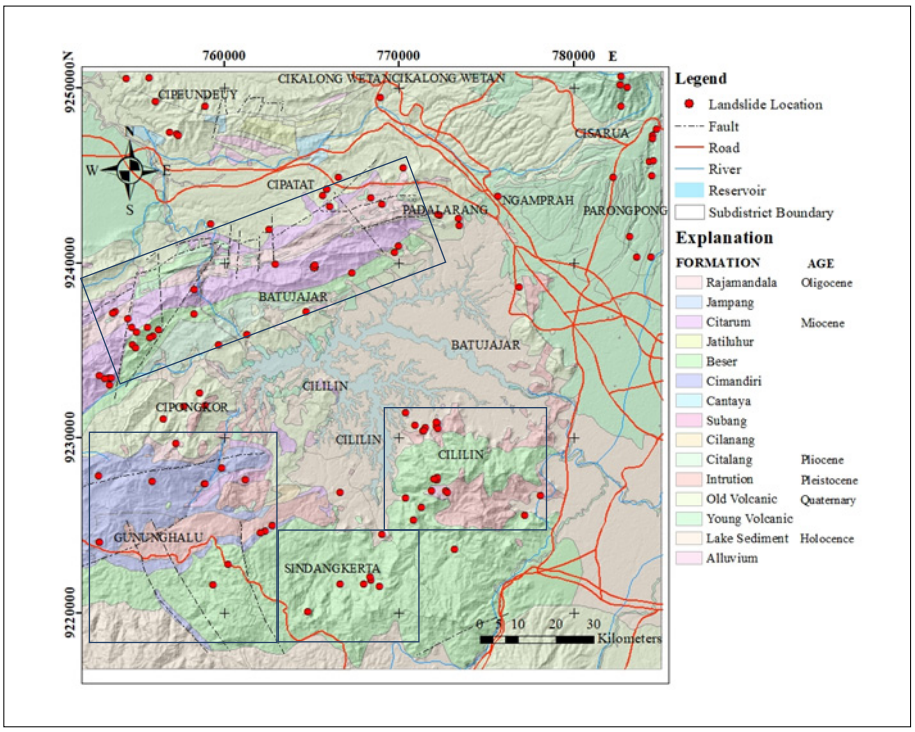

Figure 22: Relationship between the unstable hillslope area and geological structures.

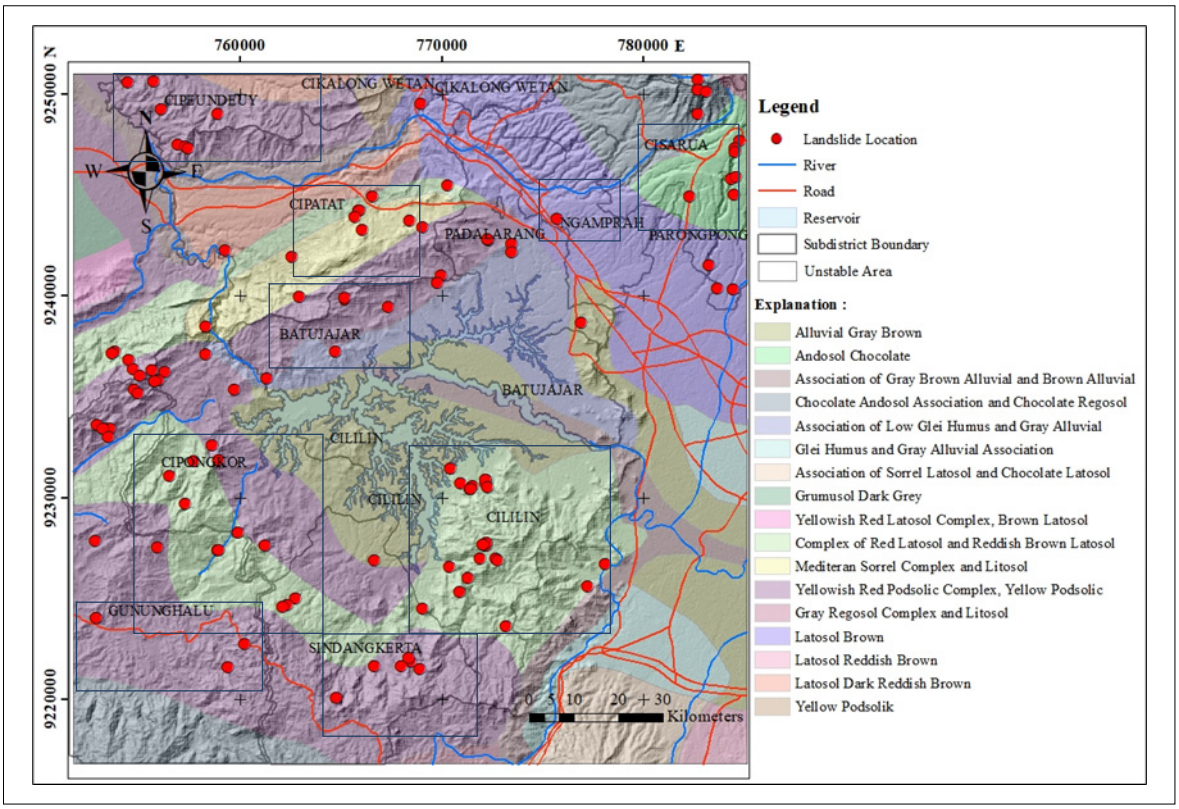

Figure 23: Distribution of soil types on unstable slopes.

influenced by specific soil parameters such as bulk density, and shear strength, among others.

The influence of soil type on landslide susceptibility in the study area is also examined. **Figure 23** shows the slope stability map of the TRIGRS model overlapped with soil type maps for the study area. According to this figure and the slope stability modelling result (see **Figure 16b**), the unstable hillslopes are mainly in hilly areas

made up of andosol soils around Cisarua, Cililin, and Cipongkor (see blue rectangle). Other landslide-susceptible areas are made up of latosol soils. Thus, the most dominant soil types sensitive to landslides are andosol and latosol soils, and both have resulted from weathering volcanic rocks. A landslide study in Karanganyar Regency Central Java also found that these two soil types are sensitive to landslides (**Priyono et al., 2023**).

4.4 Validation and evaluation of TRIGRS landslide susceptibility

Validation was performed using landslide inventory data obtained from the Center for Volcanology and Geological Hazard Mitigation data, field mapping, and landslide identification via Google Earth. This validation helps evaluate the level of influence of parameter calculations on the slope SF for each input parameter of the TRIGRS modelling. A validation process was also implemented on the modelling results of TRIGRS to evaluate the success rate of predicting slope stability and determining the model performance of rainfall-induced landslides in the study area.

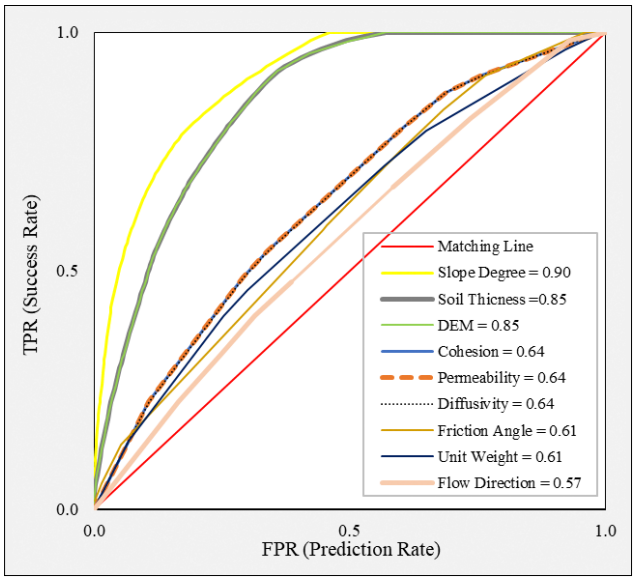

Figure 24: ROC Curve for parameters.

4.4.1 ROC curve for parameter

The ROC curve analysis shows that the AUC of each parameter value has a reasonably good validation value in modelling slope stability. The AUC value ranges from 0.57 to 0.9 for all slope stability controlling parameters. Referring to **Table 4**, slope inclination, elevation, and soil thickness are the parameters that will have a significant effect on slope stability modelling. Meanwhile, the saturated hydraulic conductivity, diffusivity, shear strength parameters, and unit weight of soils have less significant control on the modelling (see **Figure 24**). Thus, this result indicates that slope inclination, elevation, and soil thickness have a more substantial control on slope stability modelling than the shear strength parameters of the soil in the study area. In contrast, the flow direction is the lowest parameter affecting slope stability. This is because this parameter is only used in the TopoIndex program to calculate runoff routes and is not directly involved in the TRIGRS modelling to calculate the SF of the slope.

4.4.2 ROC curve for model

Figure 25 shows the ROC curves to validate the TRIGRS modelling results for each scenario using the AUC value for each rainfall duration. The models were validated by comparing the percentage of landslides generated from the TRIGRS model in scenarios A and B to the

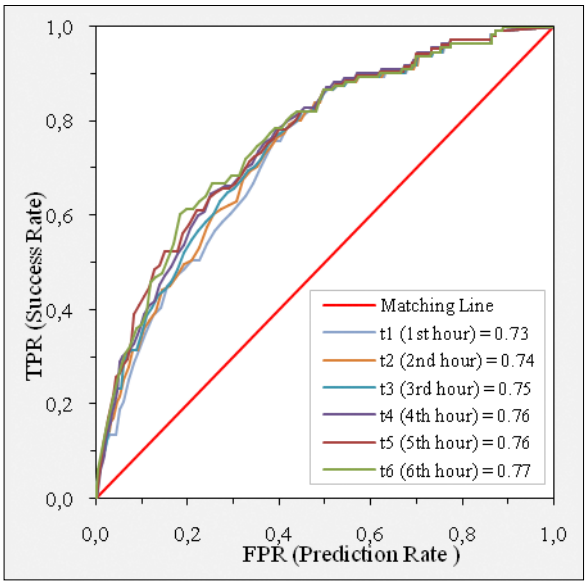

(a) AUC for each rainfall duration in Scenario A

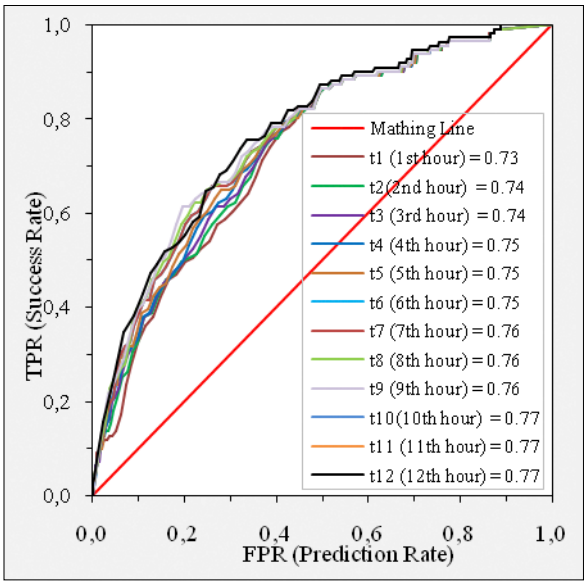

(b) AUC for each rainfall duration in Scenario B

Figure 25: ROC curve for the models for both scenarios.

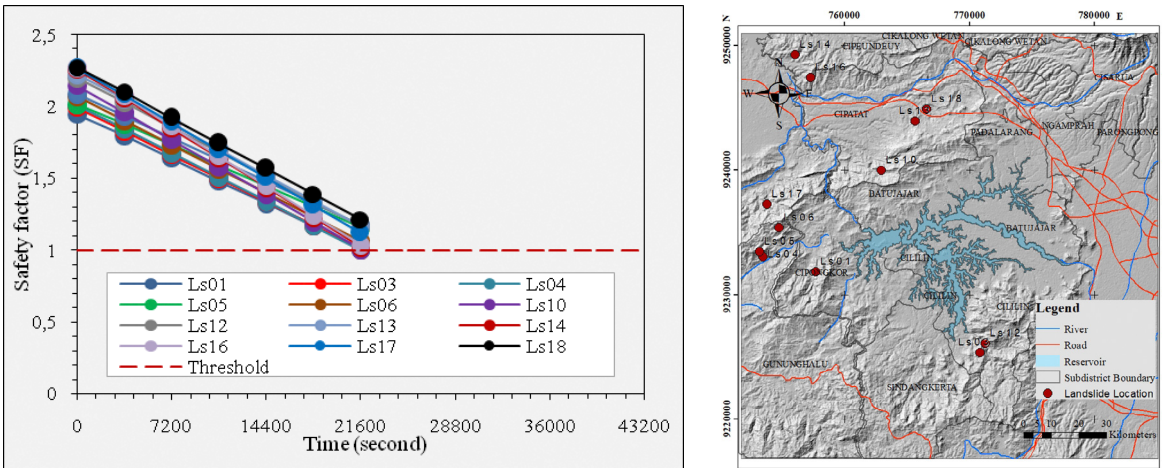

Figure 26: Variation of SF value of hillslope in scenario A for landslide locations shown in the map.

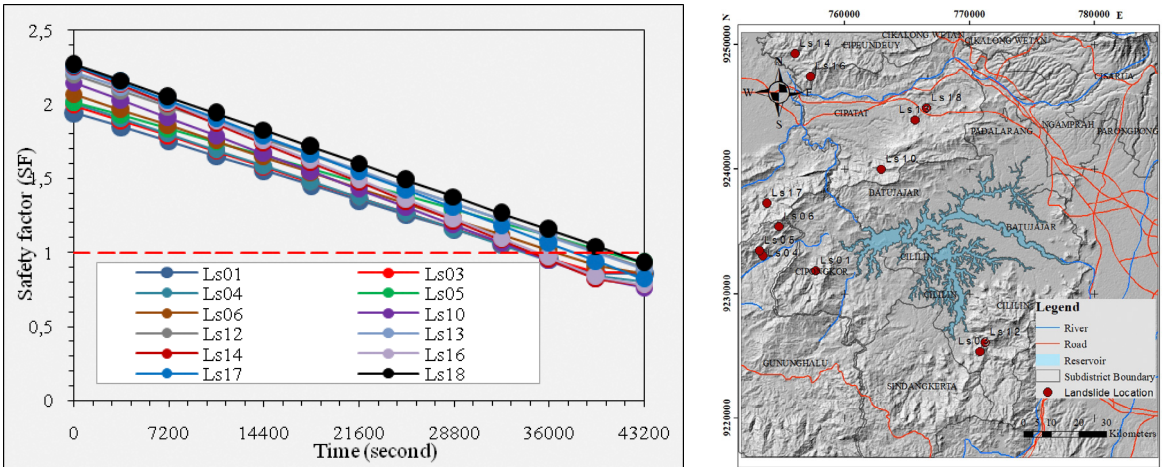

Figure 27: Variation of SF value of hillslope in scenario B for landslide locations shown in the map.

percentage of landslide inventory data. TRIGRS modelling in scenarios A and B have AUC values ranging from 0.7 to 0.77, respectively. The results of this study show that the TRIGRS modelling has fairly good accuracy in predicting rainfall-triggered hillslope instability in this study area. This study proved that rainfall intensity has a significant effect on the decreased hillslope stability.

4.4.3 Effect of rainfall characteristic on hillslope stability

Figure 26 and **Figure 27** show the graph of change in the safety factor of hillslope instability models for six historical landslide locations, from the initial condition (T0) to the final condition (T6 and T12) for each rainfall scenario. In the validation process, there are 60.7% of validated inventory data in scenario A and 63.4% in scenario B. The graphs show the safety factor decreases with the increase in rainfall duration to reach the value of less than 1.0. Thus, it is clear that long-duration rainfall of low intensity causes more hillslopes to become unstable. Thus, this study demonstrates that rainfall duration will have a more significant effect than rainfall intensity on the hillslope stability. This is because rainwater that infiltrates into the slope surface is retained longer, causing more soil layers to get saturated, and the developed pore-water pressures become higher during a longer period of rainfall. The landslide study in northwestern Colombia Andes using physically-based models indicates a greater influence of rainfall duration instead of rainfall intensity (**Aristizábal et al., 2020**). Recent landslide events that happened in the Emilia Romagna, area (Italy) in the middle of May 2023 are an example of the effect of long-duration rainfall on triggering landslides. The landslide initiation required 36 hours of antecedent rainfall with a total rainfall of 300 mm, almost the same amount of rain, that usually falls in seven months. In contrast, **Guzzetti et al. (2008)** state that average rainfall intensity is more important than rainfall duration to evaluate rainfall conditions triggering shallow landslides and debris flows.

5. Conclusions

The study presented in this paper evaluates the effect of rainfall characteristics on landslide susceptibility in

the West Java Regency through physically-based models, incorporating the intensity and duration of rainfall, as well as the spatial variability of geological conditions, morphometry, and soil parameters. The study suggests that many factors affect the stability of the hillslopes, among which the slope inclination, elevation, and soil thickness have a primary control on the hill slopes stability in the study area.

The results of TRIGRS modelling indicate that the stability of a hillslope decreases to a critical condition with the increase in rainfall duration because more rainwater will infiltrate into the hillslope and will be retained longer in the soil layer to cause more saturation of the hillslope, and hence, decrease in the hillslope stability. The evaluation of the modelling results suggests that long-duration rainfall of low intensity has a more significant impact on triggering landslides than short-duration rainfall of high intensity. Although this study has predicted the hillslope areas susceptible to rainfall-induced landslide with fair accuracy (AUC = 0.7 – 0.8), however, the current landslide susceptibility modelling is still subject to revision. More accurate landslide prediction using the TRIGRS model can be obtained when soil hydraulic and engineering properties data are available for each lithology. So, more detailed geological engineering mapping to obtain soil samples for each lithology for laboratory soil properties determination is recommended.

The results of physically-based shallow landslide prediction using the TRIGRS model provide a baseline for more detailed landslide hazard study and landslide risk assessment. In addition, establishing a landslide susceptibility map can substantially contribute to the landslide hazard mitigation strategies and landslide risk-based spatial planning in the West Bandung Regency.

Acknowledgement

The authors are sincerely thankful to the National Research and Innovation Agency of the Republic of Indonesia for providing the research funding, and the author thanks the journal's editorial staff for accepting this publication. In addition, the authors would like to acknowledge Dr. Imam A. Sadisun and Dr. Rendy D. Kartiko from the Institute of Technology of Bandung for discussing this research.

6. References

Aristizábal, E., and Sánchez, O. (2020): Spatial and temporal patterns and the socioeconomic impacts of landslides in the tropical and mountainous Colombian Andes. Disasters, 44(3), 596-618. https://doi.org/10.1111/disa.12391.

Aristizábal Giraldo, E. V., García Aristizábal, E., Marín Sánchez, R., Gómez Cardona, F., and Guzmán Martínez, J. C. (2020). Rainfall-intensity effect on landslide hazard assessment due to climate change in north-western Colombian Andes. Revista Facultad De Ingeniería Universidad De Antioquia, (103), 51–66. https://doi.org/10.17533/udea.redin.20201215.

Bai, S., Wang, J., Thiebes, B., Cheng, C., and Yang, Y. (2014): Analysis of the relationship of landslide occurrence with rainfall: a case study of Wudu County, China. Arab J Geosci., 7, 1277–1285. https://doi.org/10.1007/s12517-013-0939-9.

Baum, R. L., Savage, W. Z., and Godt, J. W. (2002): TRIGRS—a Fortran program for transient rainfall infiltration and grid-based regional slope-stability analysis, *US Geological Survey Open-File Report*, 424, 38. https://pubs.usgs.gov/

Baum, R.L., Coe, J.A., Godt, J.W., Harp, E.L., Reid, M.E., Savage, W.Z., Schulz, W.H., Brien, D.L., Chleborad, A.F., McKennan, J.P., and Michael, J.A. (2005): Regional landslide-hazard assessment for Seattle, Washington, USA. Landslides, 2, 266–279. https://doi.org/10.1007/s10346-005-0023-y.

Baum, R. L., Godt, J. W., and Savage, W. Z. (2010): Estimating the timing and location of shallow rainfall-induced landslides using a model for transient, unsaturated infiltration. Journal of Geophysical Research: Earth Surface, 115(F3). https://doi.org/10.1029/2009JF001321.

Beguería, S. (2006): Validation and evaluation of predictive models in hazard assessment and risk management, *Natural Hazards*, 37(3), 315 – 329. https://doi.org/10.1007/s11069-005-5182-6.

Bronto, S., and Langi, B. S. (2016): Geologi Gunung Padang dan sekitarnya, Kabupaten Cianjur, Jawa Barat. Jurnal Geologi dan Sumberdaya Mineral, 17(1), 37-49. Proceedings PIT IAGI Yogyakarta 2012 The 41st IAGI Annual Convention and Exhibition. *(In Indonesian)*.

Chauhan, S., Sharma, M. and Arora, M.K. (2010): Landslide susceptibility zonation of the Chamoli region, Garhwal Himalayas, using logistic regression model. Landslides, 7, 411–423. https://doi.org/10.1007/s10346-010-0202-3.

Chung, C. J. F. and Fabbri, A. G. (2003): Validation of spatial prediction models for landslide hazard mapping. Natural Hazards, 30, 451-472). https://doi.org/10.1023/B:NHAZ.0000007172.62651.2b.

Dietrich, W. E., de Asua, R. R., Coyle, J., Orr, B., and Trso, M. (1998): A validation study of the shallow slope stability model, SHALSTAB, in forested lands of Northern California. Stillwater Ecosystem, Watershed and Riverine Sciences. Berkeley, CA.

Fang, Y. S. and Chen, T. J. (1995): Modification of Mononobe–Okabe theory. Geotechnique, 45(1), 165-167. https://doi.org/10.1680/geot.1995.45.1.165.

Farahmand, A. and Agha Kouchak, A. (2013): A satellite-based global landslide model. Nat. Hazards Earth Syst. Sci., 13, 1259–1267. https://doi.org/10.5194/nhess-13-1259-2013.

Fawcett, T. (2006): An introduction to ROC analysis. Pattern recognition letters, 27(8), 861-874. https://doi.org/10.1016/j.patrec.2005.10.010.

Gorunescu, F. (2011): Data Mining Techniques and Models. In: Data Mining. Intelligent Systems Reference Library, vol 12. Springer, Berlin, Heidelberg. https://doi.org/10.1007/978-3-642-19721-55.

Guzzetti, F., Peruccacci, S., Rossi, M., Colin, P., and Stark, C.P. (2008): The rainfall intensity–duration control of shallow landslides and debris flows: an update. Landslides, 5, 3–17. https://doi.org/10.1007/s10346-007-0112-1.

Hong, M., Kim, J., and Jeong, S. (2018): Rainfall intensity-duration thresholds for landslide prediction in South Korea by considering the effects of antecedent rainfall. Landslides 15, 523–534. https://doi.org/10.1007/s10346-017-0892-x.

Hadji, R., Achour, Y., and Hamed, Y. (2018): Using GIS and RS for Slope Movement Susceptibility Mapping: Comparing AHP, LI and LR Methods for the Oued Mellah Basin, NE Algeria. In: Kallel, A., Ksibi, M., Ben Dhia, H., Khélifi, N. (eds) Recent Advances in Environmental Science from the Euro-Mediterranean and Surrounding Regions. EMCEI 2017. Advances in Science, Technology and Innovation. Springer, Cham. https://doi.org/10.1007/978-3-319-70548-4_536.

Hermawan, K., Sugianti, K., Martireni, A., Satrio, N. A., and Yunarto (2023): Spatial and Temporal Analysis Prediction of Landslide Susceptibility Using Rainfall Infiltration and Grid-based Slope Stability Methods in West Bandung area of West Java-Indonesia. In *IOP Conference Series: Earth and Environmental Science* (Vol. 1173, No. 1, p. 012031). IOP Publishing. https://doi.org/10.1088/1755-1315/1173/1/012031.

Huang, L. J. and Lin, X. S. (2002): Study on landslide related to rainfall, Journal of Xiangtan Normal University. 24 55–62.

Iverson, R. M. (2000): Landslide triggering by rainfall infiltration. Water Resour. Res., 36 1897–1910. https://doi.org/10.1029/2000WR900090.

König, T., Kux, H. J., and Corsi, A. C. (2021): Shalstab and TRIGRS: Comparison of Two Models for the Identification of Landslide-prone Areas.

Kawagoe, S., Kazama, S., and Sarukkalige, P. R. (2010): Probabilistic modelling of rainfall induced landslide hazard assessment, Hydrology and Earth System Sciences, 14, 1047–1061. https://doi.org/10.5194/hess-14-1047-2010.

Koesmono, M. and Kusnama, S. N. (1996): Peta Geologi Lembar Sindang Barang and Bandarwaru. Geol. Surv. Indonesia.Bandung, *(In Indonesian)*.

Lateh, H., Tay, L. T., Khan, Y. A., Abdulbasah Kamil, A., and Azizat, N. (2013): Prediction of landslide using rainfall intensity-duration threshold along East-West Highway, Malaysia. Casp. J. Appl. Sci. Res., 2, 124–133.

Lee, S., and Sambath, T. (2006): Landslide susceptibility mapping in the Damrei Romel area, Cambodia using frequency ratio and logistic regression models. Environ Geol., 50, 847–855. https://doi.org/10.1007/s00254-006-0256-7.

Lee, S., and Pradhan, B. (2006): Probabilistic landslide hazards and risk mapping on Penang Island, Malaysia. J Earth Syst Sci., 115, 661–672. https://doi.org/10.1007/s12040-006-0004-0.

Lepore, C., Kamal, S.A., Shanahan, P., and Bras, R.L. (2012): Rainfall-induced landslide susceptibility zonation of Puerto Rico. Environ Earth Sci., 66, 1667–1681. https://doi.org/10.1007/s12665-011-0976-1.

Marin, R.J., García, E.F. and Aristizábal, E. (2021): Assessing the Effectiveness of TRIGRS for Predicting Unstable Areas in a Tropical Mountain Basin (Colombian Andes). Geotech Geol Eng 39, 2329–2346. https://doi.org/10.1007/s10706-020-01630-w.

Mehnatkesh, A., Ayoubi, S., Jalalian, A., and Sahrawat, K.L. (2013): Relationships between soil depth and terrain attributes in a semiarid hilly region in western Iran. J. Mt. Sci. 10, 163–172. https://doi.org/10.1007/s11629-013-2427-9.

Muntohar, A.S., and Liao, HJ. (2010): Rainfall infiltration: infinite slope model for landslides triggering by rainstorm. Natural Hazards 54, 967–984. https://doi.org/10.1007/s11069-010-9518-5.

Montgomery, D.R., and Dietrich, W.E. (1994): A physically based model for the topographic control on shallow landsliding, Water Resour. Res., 30 1153–1171. https://doi.org/10.1029/93WR02979.

Mugagga, F. V., Kakembo, V., Buyinza, M. (2011): A characterization of the physical properties of soil and the implications for landslide occurrence on the slopes of Mount Elgon, eastern Uganda. Journal of the International Society for the Prevention and Mitigation of Natural Hazards, ISSN 0921-030X. https://doi.org/10.1007/s11069-011-9896-3.

Nefeslioglu, H. A., and Gokceoglu, C. (2011): Probabilistic risk assessment in medium scale for rainfall-induced earthflows: Catakli catchment area (Cayeli, Rize, Turkey). Mathematical Problems in Engineering, 2011. https://doi.org/10.1155/2011/280431.

Pack, R. T., Tarboton D. G., and Goodwin, C. N. (1998): The SINMAP Approach to Terrain Stability Mapping, in D. Moore and O. Hungr (eds), 8th Congress of the International Association of Engineering Geology, Vancouver, British Columbia, Canada 21-25 September 1998, A. A Balkema, Vol. 2: Engineering geology and natural hazards. 1157-1166.

Park, D. W., Nikhil, N. V., and Lee, S. R. (2013): Landslide and debris flow susceptibility zonation using TRIGRS for the 2011 Seoul landslide event, Natural Hazards and Earth System Sciences, 13(11), 2833 – 2849. https://doi.org/10.5194/nhess-13-2833-2013.

Polemio, M., and Petrucci, O. (2000): Rainfall as a landslide triggering factor an overview of recent international research. Landslides in research, theory, and practice. Thomas Telford, London. Pp 1219-1226. ISBN 978-0727734631.

Priyono, Triatmojo, S., Rahayu (2023): Mitigation of landslide prone areas in anticipation of climate change impacts, Journal of Multidisciplinary Research, 2 (1), 32 – 46. https://doi.org/10.56943/jmr.v2i1.277.

Saadatkhah, N., Kassim, A. and Lee, L.M. (2015): Hulu Kelang, Malaysia regional mapping of rainfall-induced landslides using TRIGRS model. Arab J Geosci 8, 3183–3194. https://doi.org/10.1007/s12517-014-1410-2.

Saulnier, G. M., Beven, K., and Obled, C. (1997): Including spatially variable effective soil depths in TOPMODEL. Journal of Hydrology, 202(1-4), 158-172. https://doi.org/10.1016/S0022-1694(97)00059-0.

Schilirò, L., Cevasco, A., Esposito, C., and Mugnozza, G. S. (2018): Shallow landslide initiation on terraced slopes: inferences from a physically based approach. Geomatics, Natural Hazards and Risk, 9(1), 295-324. https://doi.org/10.1080/19475705.2018.1430066.

Simoni, S., Zanotti, F., Bertoldi, G., and Rigon, R. (2008): Modelling the probability of occurrence of shallow landslides and channelized debris flows using GEOtop-FS. Hydrological Processes: An International Journal, 22(4), 532-545. https://doi.org/10.1002/hyp.6886.

Silitonga, P. H. (1973): Peta Geologi Lembar Bandung, Jawa, skala 1: 100.000, Direktorat Geol. Bandung, *(In Indonesian)*.

Sudjatmiko, (1972): Peta Geologi Lembar Cianjur, skala 1: 100.000. Pusat Penelitian and Pengembangan Geologi. *(In Indonesian)*.

Sugianti, K., Mulyadi, D., and Sarah, D. (2014): Pengklasan tingkat kerentanan gerakan tanah daerah Sumedang Selatan menggunakan metode Storie. Riset Geologi dan Pertambangan, 24(2), 93-104. http://dx.doi.org/10.14203/risetgeotam2012.v22.62. *(In Indonesian)*.

Sugianti, K., Sadisun, I. A., and Kartiko, R. D. (2022): Analysis of maximum-rainfall-infiltration-induced slope stability using the transient rainfall infiltration and grid-based regional slope-stability model in Cililin West Java, Indonesia. Indonesian Journal on Geoscience, 9(2) 263–278. https://doi.org/10.17014/ijog.9.2.263-278.

Sugianti, K., Sukristiyanti, S., and Tohari, A. (2016): Model kerentanan gerakan tanah wilayah Kabupaten Sukabumi secara spasial and temporal. J. Ris. Geol. and Pertamb., 26, 117. http://dx.doi.org/10.14203/risetgeotam2016.v26.270. *(In Indonesian)*.

Turner, A.K. (2018): Social and environmental impacts of landslides. Innov. Infrastruct. Solut., 3, 70. https://doi.org/10.1007/s41062-018-0175-y.

Tohari, A., Sugianti, K., and Hattori, K. (2013): Monitoring and Modelling of Rainfall-Induced Landslide in Volcanic Soil Slope. In: Margottini, C., Canuti, P., Sassa, K. (eds) Landslide Science and Practice. Springer, Berlin, eidelberg. https://doi.org/10.1007/978-3-642-31445-2_66.

Tohari, A. (2018): Study of rainfall-induced landslide: a review. In IOP Conference Series: Earth and Environmental Science. IOP Publishing, Vol. 118, No. 1, p. 012036. https://doi.org/10.1088/1755-1315/118/1/012036.

Tran, T., Lee, G., An, H. and Kim, M., (2017): Comparing the performance of TRIGRS and TiVaSS in spatial and temporal prediction of rainfall-induced shallow landslides. Environ Earth Sci., 76, 315 https://doi.org/10.1007/s12665-017-6635-4.

Zung, A.B., Sorensen, C.J., Winthers, E., (2009): Landslide soils and geomorphology in Bridger/Teton Forest Northwest Wyoming. Physical Geography, 30(6), 501–516. https://doi.org/10.2747/0272-3646.30.6.501.

Zhao, H., Yao, L., Mei, G., Liu, T., and Ning, Y.A. (2017): Fuzzy Comprehensive Evaluation Method Based on AHP and Entropy for a Landslide Susceptibility. Map. Entropy. 19(8):396. https://doi.org/10.3390/e19080396.

Zhuang, J., Peng, J., Wang, Y., Iqbal, J., Wang, Y., Li, W., Xu, Q., and Zhu, X., (2017): Prediction of rainfall-induced shallow landslides in the Loess Plateau, Yan'an, China using the TRIGRS model, Earth Surf. Process and Landforms, 42 (6), 915–927. https://doi.org/10.1002/esp.4050.

URL: https://tanahair.indonesia.go.id/demnas/#/demnas (accessed 22th December 2022).

URL: https://dibi.bnpb.go.id/home/index2 (accessed 8th January 2022).

SAŽETAK

Utjecaj geoloških i oborinskih uvjeta na analizu stabilnosti padina u modeliranju plitkih klizišta korištenjem TRIGRS modela

Provincija Zapadna Java ima visok potencijal za podložnost klizanju. Regija West Bandung u Zapadnoj Javi područje je s čestom pojavom klizišta koja su izazvana oborinskim događajima. Klizišta inicirana oborinom u istraživanome području dogodila su se 165 puta tijekom posljednjih 10 godina. Predviđanje pojave klizišta u ovoj regiji zahtijeva poznavanje faktora koji utječu na stabilnost padine. Ciljevi su ovoga rada: (1) procijeniti parametre koji utječu na stabilnost padine, (2) odrediti oborinske uvjete koji utječu na stabilnost padine i (3) procijeniti učinkovitost TRIGRS modeliranja. U okviru ovoga istraživanja primijenjena je deterministička metoda korištenjem TRIGRS modela u svrhu analize utjecaja intenziteta jednodnevne oborine koja je prethodila pojavi nestabilnosti na padini. Parametri korišteni u ovome istraživanju temelje se na terenskim istraživanjima, geološkim i topografskim kartama, inženjerskim svojstvima tla te povijesnim podatcima o oborinama. Učinak intenziteta jednodnevne prethodne oborine razmatran je u dvama scenarijima, tj. da je oborina trajala 6 sati i 12 sati. Rezultati modeliranja pokazali su da na stabilnost padina u istraživanome području utječu mnogi čimbenici poput brežuljkaste morfologije, strmih padina, niske posmične čvrstoće materijala, trošenja vulkanskih stijena i gustoće lineamenata geoloških struktura. Rezultati modeliranja također pokazuju da su pojave klizišta u istraživanome području inicirane dugotrajnim prethodnim oborinama. Na temelju ROC analize može se zaključiti kako rezultati TRIGRS modela korišteni u svrhu modeliranja stabilnosti padine dobro koreliraju sa stvarnim pojavama klizišta.

Ključne riječi:
klizište, prethodna oborina, Gumbelova metoda, stabilnost padine, TRIGRS model

Authors' contribution

Sugianti Khori (1) (M.T., junior researcher, engineering geology) initialized ideas, performed the fieldwork, analyzed the field data, and performed the modelling and presentation of the results. **Tohari Adrin (2)** (Dr., senior researcher, geotechnical engineering) performed the fieldwork, and laboratory soil mechanical property testing and analyses.